

Dissipation in Microinhomogeneous Solids: Inherent Amplitude-Dependent losses of a Non-Hysteretical and Non-Frictional Type

V. Zaitsev*, P. Sas

Katholieke Universiteit Leuven, Mechanical Engineering Department, Celestijnenlaan 300 B, B-3001, Heverlee, Belgium

Summary

A nonlinear, non-hysteretical and non-frictional mechanism of amplitude-dependent losses typical of microinhomogeneous media is proposed. This mechanism requires neither quasistatic hysteresis at the defects, nor friction-type losses such as slip at the defect's interface or another nonlinear viscosity. It is shown that inherent amplitude-dependent macroscopic attenuation in microinhomogeneous solids also occurs due to combined action of two factors, (i) purely linear (viscous-like or thermal) losses at the defects and (ii) elastic nonlinearity which is typical of such defects as cracks, intergrain contacts, etc. In particular, the defect nonlinearity of a hysteretical type also influences the resultant macroscopic amplitude-dependent attenuation via this mechanism. However, this contribution of the hysteretic nonlinearity is not related to the non-zero square of the hysteresis "stress-strain" loop, and is not associated with conventional hysteretical losses. Therefore, in a hysteretical material, these essentially different mechanisms may exhibit themselves either simultaneously or separately depending on the particular type of the nonlinear effect. For example, the role of both conventional hysteretical and the mentioned non-hysteretical nonlinear losses is comparable in case of self-action of a tonal wave, but the non-hysteretical mechanism may dominate in the special case of interaction of two different waves. The case of a solid containing isotropically oriented highly compliant microinhomogeneities is analysed as an important instructive example. Complementary nonlinearity-produced variations in the elastic moduli and in the decrements are evaluated for the longitudinal, the Young (rod) and the transversal elastic waves. Inter-relationships of the microstructure of a solid, its elastic and dissipative properties are pointed out and the relevance of the model implications to published and own experimental observations is discussed. The obtained results allow for prediction of the amplitude-dependent absorption and of the complementary change in elastic parameters for microinhomogeneous materials without detailed knowing viscoelastic properties of the defects. The model is applicable to a wide class of materials, such as rocks, concretes and other microinhomogeneous solids.

PACS no. 43.25.Dc, 43.25.Ed, 43.25.Lj, 43.35.Cg, 91.60.Lj

1. Introduction. Different mechanisms of amplitude-dependent losses

The last 10–15 years are marked by growing interest to studies of nonlinear effects exhibited by elastic waves propagating in so-called microinhomogeneous media [1–18]. This class comprises a wide variety of apparently different materials such as rocks, concrete and similar construction materials, grainy media, polycrystalline metals, etc. In many cases those media are characterized by anomalously high elastic nonlinearity compared to "normal" homogeneous solids such as single crystals or amorphous materials like defect-less glass. In the same microinhomogeneous solids, besides the pronounced elastic nonlinearity, acoustic wave dissipation is also significantly increased in magnitude, while functionally their absorption coefficient is approximately linearly proportional to the wave frequency in contrast to the quadratic-in-frequency law typical for "normal" viscous absorption [19–23]. Another interesting feature of losses in microinhomogeneous solids is their pronounced dependence on the wave amplitude [1, 5, 7, 18, 23–26]. In some cases the complementary nonlinear elasticity and the amplitude-dependent losses could be described by phenomenological stress-strain dependencies of hysteretical types, for example, to account for the

effects of nonlinear resonance frequency shift to lower frequencies and of the accompanying decrease in the resonator quality factor [5, 7, 18].

On the other hand, in a number of experiments with similar (or even the same) samples of microinhomogeneous solids, the material nonlinearity apparently manifested itself in almost purely dissipative manner, for example, in experiments on damping of an ultrasonic signal under the action of another, lower-frequency, acoustic wave [27–29, 51, 54]. In particular, it was mentioned that the relative change in absorption of the probe ultrasonic pulse under the action of the other strong ("pump") wave could reach dozens of percents, while the change in the pulse propagation time was hardly detectable. These results could not be explained by the hysteretic nonlinear terms and required to introduce amplitude-dependent losses in the macroscopic state equation of the medium [27–33]. However, in the phenomenological form, either hysteretical or alternative nonlinear-dissipative phenomenological approximations of state equations could not clarify the relationship between the physical microstructural features of the material and its acoustical properties, and the question on physical mechanisms of the microstructure-induced nonlinearity remained open.

The comprehension of this problem is of high importance for exploitation of the nonlinear acoustic effects in diagnostic applications, which seems to be very attractive, because "structural sensitivity" of both the dissipative and elastic (reactive) nonlinear effects is often drastically higher as com-

Received 12 January 1999,
accepted 23 May 2000.

* Also at the Institute of Applied Physics RAS, 46 Uljanova Str., Nizhny Novgorod, 603600, Russia

pared with linear acoustic manifestations that are conventionally used in acoustical diagnostics.

Recently, a series of papers was published [34–40] in which the elastic (both linear and nonlinear) and linear dissipative material properties were considered from a unified point of view in the framework of an instructive model of a microinhomogeneous solid. Those anomalous (compared to homogeneous materials) properties were consistently considered as complementary manifestations of material microdefects which are significantly softer than the surrounding intact matrix material. The models [34–40] allow for determining the relationship between the material microstructure and the linear and nonlinear elastic and dissipative properties of the medium. In particular, this approach allowed for effective modelling of the anomalous increase in elastic nonlinearity together with the almost frequency-independent quality factor intrinsic to the majority of microinhomogeneous solids. In the mentioned papers, however, the analysis was restricted to the cases of the linear absorption and purely elastic nonlinearity. The present paper further develops this approach. An explanation is proposed for amplitude-dependent losses in microinhomogeneous solids, which requires neither nonlinear viscosity (friction), nor quasistatic hysteresis at the defects, and can either accompany conventional hysterical losses or act independently.

Before directly turning to the consideration of the mentioned mechanism, it is important to note that the terminology related to the rapidly developing nonlinear acoustics of microinhomogeneous media is not yet generally accepted, which may cause confusion concerning even basic terms. For example, recently the terms "mesoscopic elasticity" and "mesoscopic material" were introduced (e.g., review [18]) in addition to the older terms "microinhomogeneous materials" and "microstructural nonlinearity" (e.g. review [5]), which are used in this paper, and which relate to exactly the same class of materials and phenomena. Another confusing example is the use of expressions "quadratic" and "cubic" nonlinear terms. They may mean the same being defined either using the power expansion of the stress-strain relations [17] or the elastic energy density [18]. Besides, this field of research is strongly influenced by such disciplines as nonlinear optics, nonlinear seismics, mechanics, material science, etc., for which the terminological and conceptual differences are rather significant. Therefore, in order to avoid possible misunderstanding or confusion in the ideas and terms, we recall briefly a few important concepts and specify the corresponding terminology to be used below.

Note first, that a vast amount of research related to amplitude-dependent attenuation in microinhomogeneous solids generally accepts that this phenomenon is essentially connected to the microstructural features. Concerning particular realisations of this general idea, it is possible to divide existing approaches in two main groups corresponding to two essentially different mechanisms of the macroscopic nonlinear losses.

The first mechanism is based on the assumption of hysteresis in the stress-strain relation of the microstructural defects (for example, [5, 7, 13–18, 24] and literature herein).

Due to these hysterical losses at the defects, which are described by the non-zero area of defect's hysteresis loop on the stress-strain plane, the macroscopic losses in the material exhibit amplitude-dependence. Different measures of losses may quantitatively characterise this effect; for example, quality factor Q of the material, or the decrement $\theta = \pi/Q$, or the attenuation coefficient may be used [24]. Particular physical (at the atomic-level) origin of the hysteresis may be different (adhesion at interfaces, dislocation movement, etc.), but the most important common distinction of hysteresis of any nature is the non-zero area of the macroscopic stress-strain loop.

The second essentially different mechanism is based on the assumption of some friction (or, more general, a nonlinear viscosity for which the dry friction is a special case) between defect's edges (at cracks, intergrain contacts, etc.) [21, 24, 25, 27, 32, 33, 41, 42]. In certain cases, for example, for friction with stick-slip, the stress-strain curve may also exhibit quasistatic loops with a non-zero area. The latter means that such cases may be reduced to the hysterical type and the losses may be considered in terms of hysteresis of frictional origin [24]. However, in many other cases, e.g., when the viscous (frictional) force at the defect depends nonlinearly on the velocity of defect's strain variation, there is no quasistatic hysterical "stress-strain" curve with non-zero area. Nevertheless, the macroscopic attenuation in the material will exhibit amplitude-dependence of the essentially non-hysterical origin [27, 28, 31–33, 41].

In this paper we suggest another mechanism which cannot be reduced neither to the hysterical, nor to the nonlinear-frictional mechanisms mentioned above. It implies the following properties of the defects: (i) conventional linear viscous-like losses and (ii) amplitude dependence of the defects' elastic parameters, which is typical of cracks, contacts, etc. (in other words, the elastic nonlinearity of the defects [12, 43, 44]). It is shown below that the combined influence of these two factors also results in the macroscopic amplitude-dependent attenuation. The amplitude dependence of defect elasticity may originate, in particular, not only from the purely elastic nonlinearity, but also from a hysterical nonlinearity of the stress-strain relation of the defects. Nevertheless, it is incorrect to claim that in the latter case the new mechanism becomes hysterical, because the main feature of hysteresis, the non-zero area of the stress-strain loop, is not essential for the third mechanism at all. Only the nonlinearity of defect's elastic properties is essential, and this feature is common for both hysterical or purely elastic nonlinearities. This difference between various mechanisms should be clearly distinguished: not all effects occurring in hysterical materials are of essentially hysterical origin.

This resemblance and difference between the mechanisms should not be confused, which is especially important for interpretation of experimental results. Indeed, it is well known that experiments normally indicate that real defects exhibit not purely elastic, but just hysteretic nonlinearity [24, 5, 7, 11, 18]. This means that in real solids, the formulated non-hysterical mechanism may be accompanied by amplitude-dependent attenuation due to conventional, essentially hys-

teretical losses. However, in some special cases it is possible to distinguish manifestations of these different mechanisms, and the non-hysteretic mechanism may dominate. The corresponding examples are discussed in the experimental part of the paper.

Another important issue, which also may cause confusion when interpreting experiments, is the necessity to clearly distinguish local and non-local effects. From this point of view, all three above mechanisms influence local properties of the microinhomogeneous material. However, besides the local change in material properties due to either hysteretical or the other nonlinear-attenuation mechanisms in microinhomogeneous materials, additional influence of essentially spatial features of nonlinear interactions may result in apparently similar effects. In this context, paper [41] demonstrates that hysteretical nonlinear terms retained in the wave equation yield another interesting prediction: the possibility of amplification of a weak wave propagating in the opposite direction to the second strong wave. It is pointed out in [41] that this effect is due to the energy synchronously scattered from a strong wave propagating in the opposite direction to the weak one, since the interacting waves create a kind of a dynamic diffraction "grating" due to the material nonlinearity. Synchronous interactions of such type are also well known in optical dynamic holography [45] for materials which exhibit cubic (that is odd-type) reactive nonlinearity. The hysteretical term considered in paper [41] is also the nonlinearity of the odd-type, which provides conditions for synchronous interaction of the counterpropagating waves. By analogy with the optical phenomena, the results presented in [41] for waves of identical frequency, may be extended for the cases of different frequencies, copropagating and standing waves, and yield other interesting predictions. However, we point out that the non-zero area of the hysteretic loop is not crucial for such a synchronous scattering, and, therefore, although the effect is predicted in [41] for the hysteretical medium, the nature of the phenomenon is not essentially hysteretic.

Concluding we stress once again that one should be rather careful when interpreting experimental effects related to apparently amplitude-dependent attenuation (or amplification in some cases), whether one or another mechanism is behind the experimental observation. Actually real materials may exhibit effects that are formed by different mechanisms simultaneously. Moreover, the discrimination and interpretation of the effects may be complicated due to additional influence of resonances in samples of finite length or by space-time non-local effects as in the above discussed case of interaction of counterpropagating waves. Concerning materials with hysteresis, it is also necessary to clearly distinguish whether the particular effect is essentially hysteretic or non-hysteretic (that is the non-zero area of the quasistatic stress-strain loop is crucial for the effect or not). To the authors' knowledge, these distinctions were not enough discussed in the pertinent publications, so we felt the necessity to address these questions before turning directly to the formal consideration of the qualitatively formulated non-hysteretical and non-frictional "third mechanism" of macroscopic amplitude-dependent attenuation in microinhomogeneous materials.

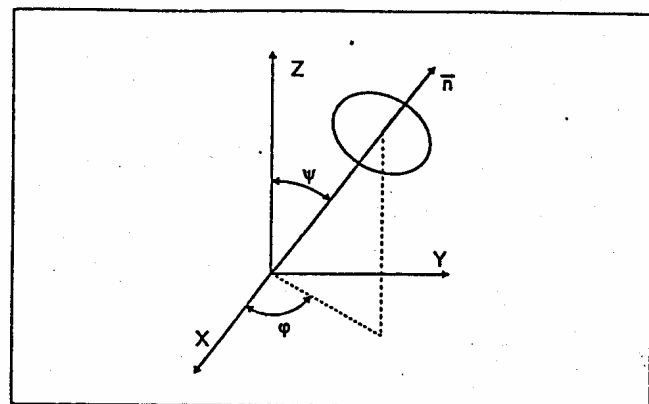


Figure 1. Spatial orientation of a defect.

The suggested mechanism yields a number of consequences allowing to discriminate it experimentally from the other mechanisms, and to account for experimentally observed effects of nonlinear-dissipative character [27–32], which could not be attributed to hysteretical losses.

2. Main features of the material microstructure

As a basis for the formulation of the new mechanism of the amplitude-dependent losses, a brief outline of the medium model together with the main results obtained for linear elastic/dissipative properties is recalled following paper [40]. The model of a microstructured medium implies that the solid matrix contains some defects-inclusions (grains, cracks, etc.) whose scale is larger than the atomic size, but small compared to the acoustic wavelength and whose compliance (softness) is much higher as compared to the surrounding defect-free material. Due to the highly increased strain and the velocity of strain changes, the volume density of the elastic energy and its dissipation rate are both significantly (by several orders of magnitude) increased at the soft defects compared to the surrounding homogeneous matrix material. It was argued in paper [40] that in most solids whose Poisson's ratio γ is not close to the "liquid" limit $\gamma = 0.5$, the highly compliant defects can be approximated by planar objects (as shown in Figure 1 for one of the defects whose spatial orientation is determined by angles ψ and φ).

The defects are assumed to be isotropically oriented in space, so that the material is considered as average-isotropic within volumes containing large amounts of the defects. The inter-defect distance is supposed to be significantly larger than the defect diameter. This condition allows one to consider the stress applied to a defect as given and makes it possible to neglect the perturbations caused by other defects. It is also assumed that the characteristic spatial scale of the average stress field (i.e., the length of an elastic wave) is significantly larger than the inter-defect distance.

Concerning the elastic properties of such inclusions, it was argued in [40] that the planar defects should be highly compliant with respect to stress applied along the axis normal to the defect plane (see Figure 2a), while the defect strain due

to compression in the in-plane direction (see Figure 2b) is much smaller and is of the same order of magnitude as in the intact material. Analogously, in some cases the defects can be highly compliant with respect to a shear in-plane stress (see Figure 2c), while in response to a shear stress applied in the normal direction (see Figure 2d) the defect compliance is comparable to that of the intact matrix material. In order to quantitatively characterize defect's compliance in response to normal stress σ_n and to shear stress σ_τ in the in-plane direction, small parameters $\zeta \ll 1$, $\zeta \in [0, 1]$ and $\xi \ll 1$, $\xi \in [0, 1]$ are introduced which relate the effective moduli E_d and G_d of the defects with Young's modulus E and shear modulus G for the matrix material:

$$E_d \equiv \zeta E, \quad (1)$$

$$G_d \equiv \xi G. \quad (2)$$

In particular cases for which models are available (e.g., for cracks modeled by penny-like cuts [46] or by more sophisticated models [42, 43]), the compliance parameters can be related to defect's dimensions. Otherwise, for our purposes it is enough to use the phenomenologically introduced elastic characteristics ζ and ξ . In addition, the defects are characterized by effective viscous parameters g_1 and g_2 with respect to their normal and shear deformation. For a defect with a given surface area S and initial thickness $L \ll \sqrt{S}$, the normal component of stress σ_n (see Figure 2a), in terms of the introduced notations, is related to the variation of the defect thickness X_n by the following equation:

$$S\sigma_n = SE_d \frac{X_n}{L} + g_1 \frac{dX_n}{dt} \equiv S\zeta E \frac{X_n}{L} + g_1 \dot{X}_n, \quad (3)$$

where $dX_n/dt \equiv \dot{X}_n$. Under the action of the in-plane shear (tangential) stress σ_τ (Figure 3c) the shear (tangential) deformation X_τ of a defect is described by a similar equation of state (notations are clear by analogy with equation 3):

$$S\sigma_\tau = SG_d \frac{X_\tau}{L} + g_2 \frac{dX_\tau}{dt} \equiv S\xi G \frac{X_\tau}{L} + g_2 \dot{X}_\tau. \quad (4)$$

Note that physically the effective viscosity of the defects most likely is associated with thermal losses which are essentially increased at the defects due to local gain of strain and increased thermal gradients in the their vicinity [47, 48], and, in presence of a fluid inside the defects, conventional viscous losses may occur. For the present analysis it is quite enough to take these losses into account via the viscous coefficients $g_{1,2}$ as their atomic-level origin and the exact magnitudes are of secondary importance for the resultant macroscopic absorption [40].

The orientation of the defects with different given compliance is characterized by a distribution function $v(\psi, \varphi, \zeta, \xi)$ which depends on the orientation angles ψ, φ and on the non-dimensional elastic parameters ζ, ξ . (Note, that, as it is argued in [39, 40], the distribution over viscous parameters is of secondary importance and here it may be omitted, since the below results show that in a wide frequency band the macroscopic attenuation in the material does not depend on

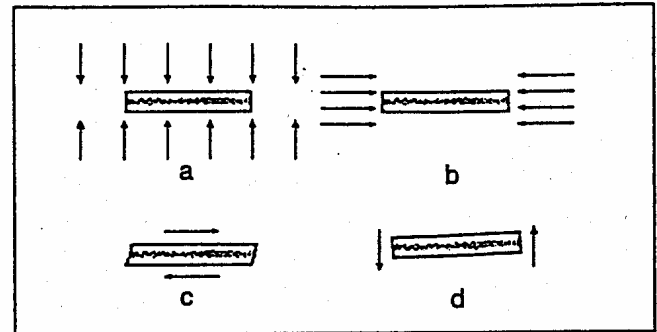


Figure 2. Schematically shown a disc-shape (planar) defect under the action of applied stress. (a) – normal compression; (b) – in-plane compression; (c) – in-plane shear stress; (d) – shear stress in normal direction.

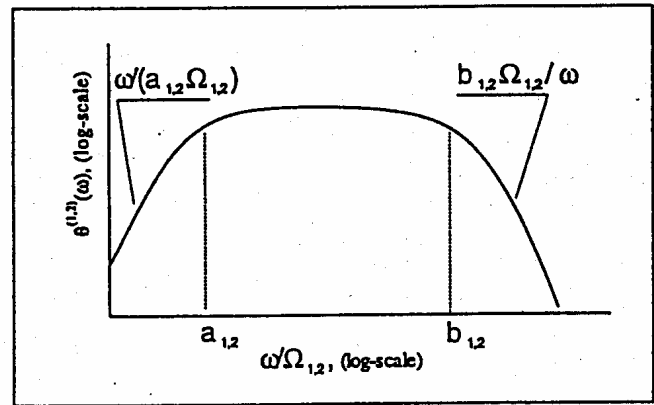


Figure 3. Schematically shown frequency dependencies $\theta^{(1,2)}(\omega)$ displaying the wide frequency band $a_{1,2}\Omega_{1,2} < \omega < b_{1,2}\Omega_{1,2}$ in which the decrement magnitude is approximately constant.

the viscosity of the defects). Further, the partial distributions $v(\zeta)$ and $v(\xi)$ over elastic parameters ζ, ξ can be introduced:

$$v(\zeta) = \int_0^{2\pi} d\varphi \int_0^{\pi} \int_0^1 v(\psi, \varphi, \zeta, \xi) \sin \psi d\psi d\xi, \quad (5)$$

$$v(\xi) = \int_0^{2\pi} d\varphi \int_0^{\pi} \int_0^1 v(\psi, \varphi, \zeta, \xi) \sin \psi d\psi d\xi. \quad (5)$$

For example, $v(\zeta)d\zeta$ characterizes the relative volume content (their volume per unit volume of the material) of arbitrary oriented defects whose parameter ζ of the normal compliance belongs to the region $[\zeta, \zeta + d\zeta]$. Partial distribution $v(\xi)$ has the similar meaning. Therefore the total defect content v_t is determined by the following expression:

$$v_t = \int v(\zeta) d\zeta = \int v(\xi) d\xi \quad (6)$$

$$= \int_0^{2\pi} d\varphi \int_0^{\pi} \int_0^1 \int_0^1 v(\psi, \varphi, \zeta, \xi) \sin \psi d\psi d\xi d\zeta.$$

Note that according to the above accepted assumptions, the total defect content is small: $v_t \ll 1$. It is important that the

distributions over the elastic parameters $v(\zeta)$, $v(\xi)$ and the distribution $v(\psi, \varphi)$ over the spatial orientations are essentially independent, so it is possible to perform the spatial-angular averaging independently for defects with different elastic parameters. In particular, for isotropic orientations, the uniform angular distribution is normalized as:

$$v(\psi, \varphi) = \frac{1}{4\pi}. \quad (7)$$

3. Microstructure-induced changes in the linear elastic moduli and in the decrements: basic linear approximation

Here we briefly summarize the main results on the microstructure-produced variations in the material elastic moduli and in the decrements for different types of waves which are obtained in [40] in the linear case and which are essential for further discussion of nonlinear effects. The non-dimensional decrement θ has the conventional meaning, and is related to the wave absorption coefficient α as $\theta = \alpha\lambda = \alpha c/f$, where λ is the wavelength of the elastic wave of a given type, f is its frequency, and c is its velocity. The same decrement can be also expressed via the ratio $\theta = W_{\text{dis.}}/(2W_{\text{el.}})$, where $W_{\text{dis.}}$ means the wave energy losses in a unit volume during one period of a harmonic wave, and $W_{\text{el.}}$ is the maximal value of density of the elastic energy of the wave motion.

Using the energy balance approach, the following expressions for moduli $E_{\text{eff.}}$ for the Young (rod) wave, $G_{\text{eff.}}$ for the shear wave and $M_{\text{eff.}}$ for the longitudinal wave were derived:

$$\tilde{E} = \frac{E_{\text{eff.}}}{E} = \left[1 + \frac{1}{5}N_1 + \frac{5}{15}(1 + \gamma)N_2 \right]^{-1}, \quad (8)$$

$$\tilde{G} = \frac{G_{\text{eff.}}}{G} = \left[1 + \frac{2}{15}N_1/(1 + \gamma) + \frac{5}{5}N_2 \right]^{-1}, \quad (9)$$

$$\begin{aligned} \tilde{M} = \frac{M_{\text{eff.}}}{M} = & \left[1 + \frac{4}{15}N_1/(1 - \gamma) \right. \\ & \left. + \frac{5}{15}N_2(1 + \gamma)/(1 - \gamma) \right]^{-1} \quad (10) \\ & \cdot \left[\left(1 + \frac{2}{15}N_1/(1 + \gamma) + \frac{2}{5}N_2 \right) \right. \\ & \left. \cdot \left(1 + \frac{1}{3}N_1/(1 - 2\gamma) \right) \right]^{-1}. \end{aligned}$$

Here notations E , G , and M relate to the moduli for the matrix material and \tilde{E} , \tilde{G} , and \tilde{M} are the corresponding non-dimensional moduli for the microinhomogeneous medium. Parameters N_1 and N_2 in expressions (8) through (10) have the following meaning:

$$N_1 = \int v(\zeta)/\zeta d\zeta, \quad N_2 = \int v(\xi)/\xi d\xi. \quad (11)$$

Below they are called the effective defect densities. Physically, as it is clear from equations (11), parameters N_1 and N_2 are determined jointly by the compliance of the defects and their concentration. In case of identical defects with fixed values of compliance parameters ζ and ξ , the distributions have the form of delta-functions, so that:

$$N_1 = v_t/\zeta, \quad N_2 = v_t/\xi. \quad (12)$$

However, it is natural to assume that real defects are not identical and are characterized by a wide distribution over their parameters of compliance, and it is convenient to approximate the distributions by wide II-shape functions (by analogy with papers [37–40]):

$$v(\zeta) = \begin{cases} v_0^{(1)}, & \text{when } \zeta \in [a_1, b_1], a_1 \ll b_1 \ll 1 \\ 0, & \text{when } \zeta \notin [a_1, b_1], \end{cases} \quad (13)$$

$$v(\xi) = \begin{cases} v_0^{(2)}, & \text{when } \xi \in [a_2, b_2], a_2 \ll b_2 \ll 1 \\ 0, & \text{when } \xi \notin [a_2, b_2]. \end{cases} \quad (14)$$

Therefore, total volume densities are given by expressions:

$$v_t = \int_0^1 v(\zeta) d\zeta = (b_1 - a_1)v_0^{(1)} \approx b_1 v_0^{(1)},$$

$$v_t = \int_0^1 v(\xi) d\xi = (b_2 - a_2)v_0^{(2)} \approx b_2 v_0^{(2)}. \quad (15)$$

Parameters N_1 and N_2 then obtain the following forms:

$$N_1 = v_t \ln(b_1/a_1)/b_1, \quad N_2 = v_t \ln(b_2/a_2)/b_2. \quad (16)$$

As a second result, calculating the period averaged losses $W_{\text{dis.}}$ at the visco-elastic defects due to their normal compression (decrement $\theta^{(1)}$) or shear deformation (decrement $\theta^{(2)}$), the following expressions were derived [40]:

$$\theta^{(1)}(\omega) = \pi v_0^{(1)} \frac{D_{\text{eff.}}}{E} \langle T_1^2(\varphi, \psi) \rangle \arctan \frac{\zeta}{\omega/\Omega_1} \Big|_{a_1}^{b_1} \quad (\text{"compressional" losses}), \quad (17)$$

$$\theta^{(2)}(\omega) = \pi v_0^{(2)} \frac{D_{\text{eff.}}}{E} \langle T_2^2(\varphi, \psi) \rangle \arctan \frac{\xi}{\omega/\Omega_2} \Big|_{a_2}^{b_2} \quad (\text{"shear" losses}). \quad (18)$$

Here notation $D_{\text{eff.}}$ is for one of the moduli $E_{\text{eff.}}$, $G_{\text{eff.}}$ or $M_{\text{eff.}}$ depending on the type of the considered wave. Characteristic frequencies $\Omega_{1,2}$ depend on the defects viscosity: $\Omega_1 = ES/(g_1 L)$, $\Omega_2 = ES/(g_2 L)$. Angular-averaged coefficients $\langle T_1^2(\varphi, \psi) \rangle$, $\langle T_2^2(\varphi, \psi) \rangle$ are given by the following expressions:

$$\langle T_1^2(\varphi, \psi) \rangle = \begin{cases} \frac{1}{5} + \frac{2\gamma_{\text{eff.}}}{15(1 - \gamma_{\text{eff.}})} + \frac{8\gamma_{\text{eff.}}}{15(1 - \gamma_{\text{eff.}})^2}, \\ 1/5, \\ 1/15, \end{cases}$$

$$\langle T_2^2(\varphi, \psi) \rangle = \begin{cases} \frac{2}{15} \left(\frac{1 - 2\gamma_{\text{eff.}}}{1 - \gamma_{\text{eff.}}} \right)^2 \\ 2/15, \\ 4/15, \end{cases} \quad (19)$$

for the plane longitudinal wave, for the rod (Young) wave, and for the transversal wave, respectively.

These expressions contain the effective Poisson ratio $\gamma_{\text{eff.}}$ for the microinhomogeneous material, which can be readily

obtained as a consequence of equations (8), (9), (10) for moduli $E_{\text{eff.}}$, $G_{\text{eff.}}$ and $M_{\text{eff.}}$:

$$\gamma_{\text{eff.}} = \frac{\gamma - \frac{1}{15}N_1 + \frac{2}{15}(1+\gamma)N_2}{1 + \frac{1}{5}N_1 + \frac{4}{15}(1+\gamma)N_2}. \quad (20)$$

The total losses are determined by the contributions of both decrements: $\theta(\omega) = \theta^{(1)}(\omega) + \theta^{(2)}(\omega)$. Qualitatively the frequency behavior of decrements $\theta^{(1,2)}(\omega)$ is shown in Figure 3. It is essential that in wide frequency bands $a_{1,2}\Omega_{1,2} < \omega < b_{1,2}\Omega_{1,2}$ decrements (17), (18) are approximately constant ($\theta^{(1,2)}(\omega) \approx \theta_c^{(1,2)}(\omega) = \text{const.}$), and are primarily determined by the defect densities N_1 and N_2 :

$$\begin{aligned} \theta_c^{(1)}(\omega) &= \frac{\pi^2}{2} v_0^{(1)} \bar{D} \frac{D}{E} \langle T_1^2(\varphi, \psi) \rangle \\ &\approx \frac{\pi^2}{2} \frac{N_1}{\ln(b_1/a_1)} \bar{D} \frac{D}{E} \langle T_1^2(\varphi, \psi) \rangle, \end{aligned} \quad (21)$$

$$\begin{aligned} \theta_c^{(2)}(\omega) &= \frac{\pi^2}{2} v_0^{(2)} \bar{D} \frac{D}{E} \langle T_2^2(\varphi, \psi) \rangle \\ &\approx \frac{\pi^2}{2} \frac{N_2}{\ln(b_2/a_2)} \bar{D} \frac{D}{E} \langle T_2^2(\varphi, \psi) \rangle, \end{aligned} \quad (22)$$

whereas the viscous properties ($\Omega_{1,2} = ES/(g_{1,2}L)$) are not present in expressions (21), (22), and are not essential for evaluation of the near-constant decrements. These results provide a plausible explanation for the numerous experimental data on near-constant decrements typical of many microinhomogeneous solids [19–23]. Therefore, expressions (8) through (22) allow for evaluating the microstructure-induced linear absorption, and relate its magnitude with the complementary decrease in the material elastic moduli. The corresponding detailed discussion of the linear results is given in reference [40].

As it was already mentioned in the introduction, the same microinhomogeneous solids, for which the almost frequency-independent decrement is typical, also exhibit anomalously high elastic nonlinearity, and nonlinear generalizations of the above considered model readily account for this phenomenon [31–33, 38]. This elastic nonlinearity pronouncedly manifests itself, for example, in generation of higher harmonics and softening of the material, which is rather pronounced even at small strain magnitudes $\epsilon \propto 10^{-7} \dots 10^{-6}$ [5, 7, 11, 23]. In contrast, solids with a homogeneous structure like glass (whose nonlinearity is determined by the interatomic potential) does not exhibit noticeable nonlinearity at such small strains. It is essential that just for the same strain amplitudes $\epsilon \propto 10^{-7} \dots 10^{-6}$, at which for a microinhomogeneous solid its elastic moduli exhibit pronounced decrease, the decrement also becomes amplitude-dependent, normally exhibiting significant increase [7, 18, 23–25]. These amplitude-dependent losses are traditionally attributed to adhesion-hysteretical or frictional losses at the microstructural defects [24–26]. However, as it is shown in the next sections, in microinhomogeneous solids another mechanism of amplitude-dependent losses must also occur, which implies only linear viscous-like dissipation and elastic nonlinearity occurred at the defects, and for which neither adhesion hysteresis, nor frictional losses are not crucial.

4. Amplitude-dependent variations in the elastic moduli and the decrements: formulation of the non-hysteretical mechanism

According to the summarized above expressions, the microstructure-induced variations in the material parameters are determined by the same properties of the defects both for the macroscopic elastic moduli and for the decrements. Namely, effective defect densities N_1 and N_2 are most important (see the structure of equations (8) through (10) and (21), (22)).

In the analysis of the elastic properties and of the attenuation, until now the effective densities N_1 and N_2 of the defects were considered as given following the linear model [40]. This approximation corresponds to the assumption that the amount of the defects is fixed, and the elasticity of the defects does not depend on the applied stress or, in other words, that the defects are perfectly linear. However, it is well known that microstructural defects in solids (like intergrain contacts, microcracks, etc.) are essentially nonlinear [12, 43, 44]. The linear description is only an approximation valid for small variations in the applied stress and the material strain.

Therefore, generally speaking, the elastic parameters of the defects ζ and ξ depend on the applied stress $\sigma_{\text{ext.}}$ (alternatively this dependence may be expressed via the defect deformation). To take this effect into account, the equations of state of the defects have to be complemented with nonlinear terms, for example, in the following form:

$$S\sigma_n = S\bar{\zeta}E(X_n/L)[1 + F_1(X_n/L)] + g_1\dot{X}_n, \quad (23)$$

$$S\sigma_\tau = S\bar{\xi}E(X_\tau/L)[1 + F_2(X_\tau/L)] + g_2\dot{X}_\tau. \quad (24)$$

In these equations, non-dimensional functions $F_1(\cdot)$ and $F_2(\cdot)$ characterize the deviation of the "stress-strain" relation for individual defects from the linear law. For example, when the factor $(X/L)F(X/L)$ (indexes are omitted here) is a quadratic or cubic function, the defect exhibits quadratic- or cubic-in-strain nonlinearity, respectively. Generally speaking, these functions may be hysteretical as well. Parameters $\bar{\zeta}$, $\bar{\xi}$ are the initial (unperturbed) values corresponding to the defect's elasticity in the unperturbed state, whereas the actual magnitudes of the defect's parameters of compliance depend on the defect's strain via the functions $F_{1,2}(\cdot)$:

$$\zeta(X_n/L) = \bar{\zeta}[1 + F_1(X_n/L)], \quad (25)$$

$$\xi(X_\tau/L) = \bar{\xi}[1 + F_2(X_\tau/L)]. \quad (26)$$

This amplitude-dependence of nonlinear elasticity of individual defects results in the corresponding amplitude-dependence of the effective densities $N_{1,2}$, because they depend on both the amount of the defects and their elasticity (see equations 11). Therefore, the nonlinear elasticity of the defects must influence both the elastic parameters of the material and the decrements via the amplitude dependence $N_{1,2} = N_{1,2}(\sigma_{\text{ext.}})$ (see equations (8)–(10) and (17), (18), (21), (22)).

Concerning the influence of the nonlinearity of individual defects on the macroscopic elastic nonlinearity one may refer

to papers [31–33], in which this mechanism is discussed in details in the 1D approximation, and 3D features will be considered elsewhere. In the present discussion, however, we are focused on the dissipative amplitude-dependent properties. In this context, note first that for a perturbation (wave), whose stress amplitude is small compared to the applied external quasistatic stress $\sigma_{\text{ext.}}$, the dependence $N_{1,2} = N_{1,2}(\sigma_{\text{ext.}})$ via functions $F_{1,2}(\cdot)$ corresponds to dependence of the material parameters on static (or slowly varying) external loading of the medium. This "instantaneous" dependence on a slowly varying load is one of manifestations of the material nonlinearity, and the derivative $d\epsilon/d\sigma_{\text{ext.}}$ of the wave velocity with respect to the external quasistatic stress is often used to quantify the medium elastic nonlinearity [13]; the derivative $d\theta/d\sigma_{\text{ext.}}$ may be analogously used for the dissipative nonlinearity.

Then a question arises if analogous amplitude-dependent variations in the material properties could be caused by a non-quasistatic, an oscillatory stress (e.g., stresses in a harmonical wave):

$$\sigma = \sigma_0 \cos(\omega t), \quad \epsilon = \epsilon_0 \cos(\omega t). \quad (27)$$

Evidently, if the nonlinear corrections to the defect elasticity $F_1(\cdot)$ and $F_2(\cdot)$ (see equations 25, 26) were perfectly odd functions, then the changes in defects's elasticity during positive and negative semi-cycles of the oscillatory deformation would be exactly compensated thus resulting in zero period-averaged change in material properties. However, it is well known that both the theoretical models of defects (e.g. contacts [48, 44] or cracks [43]) and the experimental data [5, 6, 16, 21–23] on medium softening at higher oscillation amplitudes indicate that defects' elastic nonlinearity $(X/L)F(X/L)$ in equations (23), (24) has an odd part (i.e. function $F(\cdot)$ has an even part), and, consequently, such a period-averaged compensation of nonlinear corrections normally does not occur and, therefore, the period-averaged density $\langle N \rangle$ must exhibit amplitude dependence:

$$\langle N \rangle = N(\sigma_0) = N(0) + \Delta N(\sigma_0). \quad (28)$$

In principle, nonlinear correction $\Delta N(\sigma_0)$ can be predicted from equations (23), (24) and (11) if we introduce explicit expressions for functions $F_{1,2}(\cdot)$ (and, if necessary, assume that the number of defects is not fixed due to fracturing and creation of new defects at strong enough stress). However, rather general and practically important conclusions can be made without specifying these functions and even without the assumption whether the number of the defects is fixed or not. Namely, we may use expressions (8)–(10) and (21), (22) with amplitude-dependent density $N = N(\sigma_0)$ to evaluate the complementary variations in the decrements and in the period-averaged material moduli (which may be verified experimentally). Such evaluation does not require an explicit form of $N(\sigma_0)$. Numerical examples of the corresponding calculations will be given in the next section.

Let us summarize now the main assumptions from which amplitude-dependent attenuation of the described above type has been predicted. The effect was inferred supposing only

conventional linear (viscous or thermal) losses and nonlinearity of elastic properties of individual defects. It is clear from equations (17) through (25) that it is the nonlinear variation in elastic parameters of the defects, which influences the rate of the conventional viscous-like energy dissipation at the defects. The variation in the elasticity of the defects and, therefore, the corresponding variation in their effective density $N(\sigma_0)$ may be produced by either hysteretic or purely elastic (non-dissipative and non-hysteretical) nonlinearity of the defects, as follows from equations (11) and (23)–(26). Therefore, the mechanism consists of the combined influence of conventional linear losses at the defects and their nonlinear elasticity. Joint effect of these factors results in amplitude-dependence of the macroscopic attenuation in the microinhomogeneous material.

Note that traditionally, the experimentally observed complementary amplitude-dependent variations of the elastic moduli and of the losses were attributed by many authors to a hysteretical nature of the material stress-strain relation [5, 7, 15, 18, 24]. Indeed, it is natural to expect appearance of a hysteresis, because partially inter-atomic bonds in the material are broken at opening of the microdefects. However, any hysteresis inherently implies both the dissipation described by the area of the hysteresis loop and the deviation from the linear elastic behavior. The hysteretical nonlinearity of the defects thus must also influence the macroscopic attenuation via the above considered mechanism (although the non-zero area of the hysteresis loop is not crucial for the effect). Therefore, the described amplitude-dependent non-hysteretical losses must occur in a hysteretical medium as well and co-exist with conventional hysteretical losses.

Concluding this section it is worth to briefly address the role of the second traditionally discussed mechanism of the amplitude-dependent attenuation, which is based on frictional stick-slip at the defects surfaces [25, 42]. Evidently, such an effect may take place in a strong wave field, however, the occurrence of this mechanism seems to be rather unlikely at moderate strains $\epsilon \propto 10^{-7} \dots 10^{-6}$ and for typical sizes of microdefects of the order of fractions of millimeter [25, 47]. Indeed, for example, the maximum slip Δu for a crack of length l is roughly of the order $\Delta u \approx \epsilon l$, and this estimate does not depend on a particular model of the crack [25]. This requires the crack's length to be too large (about $l = 1$ cm or more) to provide the interfaces slip about several atomic sizes (10^{-7} cm), which is necessary for frictional losses [25, 47]. Otherwise, for smaller defects, the necessary strain amplitude must be 1–3 orders of magnitude higher ($\epsilon \propto 10^{-5} \dots 10^{-3}$ or even more). Nevertheless, in many cases solids manifest amplitude-dependent attenuation and complementary decrease in elastic moduli even at $\epsilon \leq 10^{-7} \dots 10^{-6}$, although they did not contain such large cracks at which the frictional slip may occur [24, 25]. Thus, the slip hypothesis cannot be accepted in this case, whereas the suggested "cascade" mechanism (nonlinear elasticity + viscous losses = amplitude-dependent attenuation) can readily account for existence of the amplitude-dependent attenuation and variations of the elastic moduli at moderate strains $\epsilon \leq 10^{-7} \dots 10^{-6}$. From experimental point of view more

important is the problem of the effect separation from conventional hysteretical losses. Therefore, below we shall not return to the comparison with frictional effects, but focus on the relation of the proposed non-hysteretical and the conventional hysteretical mechanisms, since both may occur at the same experimental conditions.

5. Similarity and distinctions between amplitude-dependent losses due to hysteresis and due to the suggested non-hysteretical mechanism

According to the previous section, equations (21), (22) and (8) through (10) could be used to evaluate the corresponding variations in material elasticity and the decrement due to the dependence of the effective density of the defects ($\langle N \rangle = N(\sigma_0)$ or $\langle N \rangle = N(\varepsilon_0)$) on the wave amplitude.

Note that stronger stress may cause both the variation in elasticity of individual defects and variation in their amount, and these variations both influence $N(\varepsilon_0)$. Rigorously speaking, the decrement (see equations (21), (22)) depend on the defect distribution function not only via the effective density $N(\varepsilon_0)$, but also via the logarithmic function $\ln(b/a)$, which is also determined by the distribution of the defects over the elastic parameters. This logarithmic dependence, however, is rather weak, so that even a large variation in the ratio b/a such as $b/a \sim 10^4 \leftrightarrow 10^3$ gives only 20...30% corresponding variation in the logarithm $\ln(b/a)$. Additionally it could be argued that at moderate amplitudes ($\varepsilon \leq 10^{-6} \dots 10^{-5}$), such a strong perturbation in the defect amount is unlikely, whereas the decrement often exhibits variations of 50–100 percent [24, 7, 27], that is significantly larger than the possible correction due to variation of the slow logarithmic function $\ln(b/a)$. Bearing this in mind, for a moment we take into account only the variation of the effective defect density $N(\varepsilon_0)$ in the illustrative estimates below. By similar reasons (similar magnitude of corrections) we also neglect the correction associated with the weak logarithmic dispersion of the elastic moduli, which is due to the influence of the relaxation in the relationship between defect's deformation and the applied stress. This effect may be taken into account much like the linear dispersion of the elastic moduli [38–40], since the nonlinear and linear microstructure-induced changes in the elasticity has common origin and may be accounted for in the similar way.

In the estimate of the amplitude-dependent parameter variations, we consider the example of the defects that are highly compliant only with respect to normal stress. This assumption corresponds in our notations to the condition $N_1/N_2 \gg 1$ (cases $N_1/N_2 \sim 1$ and $N_1/N_2 \ll 1$ may be analyzed by analogy with the linear case [40], and yield the same order of the effect magnitude). Using equations (8) through (10) and (21), (22) and considering the effective defect densities as functions of the wave amplitudes $\langle N \rangle = N(\varepsilon_0) = N(0) + \Delta N(\varepsilon_0)$ we can calculate the relative nonlinear variations in the elastic wave velocities $\langle \Delta c(\varepsilon_0) \rangle / c \approx \langle \Delta D(\varepsilon_0) \rangle / 2D = (1 - \langle \bar{D}(\varepsilon_0) \rangle) / 2$ and the corresponding variation in the material decrement $\langle \Delta \theta_c(\varepsilon_0) \rangle$ as

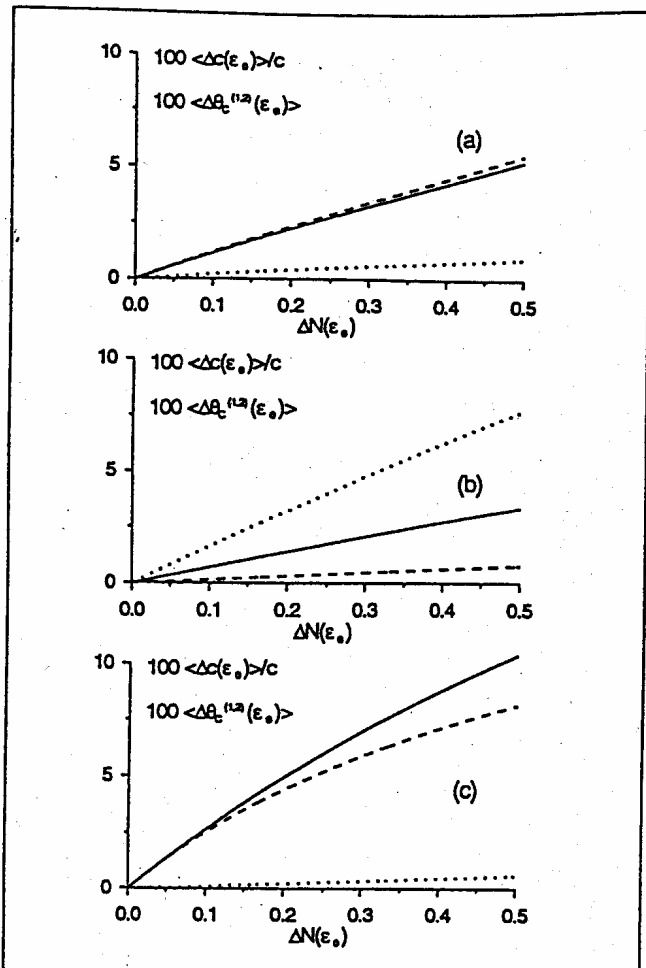


Figure 4. Examples of calculations of the period-averaged nonlinear variations in the wave velocities $100\langle \Delta c(\varepsilon_0) \rangle / c$ (the solid lines), and the corresponding variations in decrements $100\langle \Delta \theta_c^{(1)}(\varepsilon_0) \rangle$ (the dashed lines) and $100\langle \Delta \theta_c^{(2)}(\varepsilon_0) \rangle$ (the dotted lines). Parameter $N_2 = N_1/10$, Poisson's ratio $\gamma = 0.3$. (a) – Young's (rod) mode, (b) – shear wave, (c) – longitudinal wave.

functions of $\Delta N(\varepsilon_0)$. We do not need to explicitly specify the $\Delta N(\varepsilon_0)$ as is argued above. Examples of the calculations are presented in Figure 4 for the Young (rod) mode, the shear and longitudinal waves.

The plots demonstrate that the nonlinear variation in the magnitude of the decrement $\langle \Delta \theta_c(\varepsilon_0) \rangle$ may differ several times for different waves, but by the order of magnitude $\langle \Delta \theta_c(\varepsilon_0) \rangle$ is the same as the relative variation in the wave velocities (elastic moduli) $\langle \Delta c(\varepsilon_0) \rangle / c \approx \langle \Delta D(\varepsilon_0) \rangle / 2D$. However, the relative change in the decrement magnitude $\langle \Delta \theta_c(\varepsilon_0) \rangle / \theta_0$ is significantly larger than $\langle \Delta D(\varepsilon_0) \rangle / D$, because the initial decrement value $\theta_0 = \pi/Q$ is normally rather small. For example, magnitudes of the quality factor $Q = 50 \dots 300$ or higher are typical of many rocks and polycrystalline metals [19, 22, 23]. Therefore, the nonlinearity-induced relative variation in the decrement $\langle \Delta \theta_c \rangle / \theta_0$ can often be by one-two orders of magnitude larger than the relative variation in the elastic moduli $\langle \Delta D \rangle / D \approx 2\langle \Delta c \rangle / c$. Indeed, experimental data by different authors indicate that it is a typical situation: nonlinear decrease in sound velocity

of about 1...2% only is often accompanied by decrease in the quality factor by 50–100% or more (see e.g., [7, 21, 24]).

It is well known that approximately the same magnitude of the ratio between the amplitude-dependent decrement and the relative variation in the elastic moduli is a general feature of conventional hysteretical models [13, 24]. Indeed, this is quite evident physically, because the same break of inter-atomic bonds causes, on one hand, decrease in the elastic modulus $(\Delta D(\varepsilon_0))/D$ and, on the other hand, results in the hysteretic losses, which are macroscopically described by the area of the hysteresis loop. Comparing this consequence of conventional hysteretical models with the results of the calculations of the non-hysteretical amplitude-dependent variations in the decrements and elasticity presented in Figure 4, one should conclude that both mechanisms apparently predict similar effects of the same order of magnitude. This coincidence is the plausible reason why in many works there has been no report on significant discrepancy between experimental data on amplitude-dependent attenuation and hysteretical models (for example, [5, 7, 11, 18, 24] and references herein).

The question arises if it is at all possible to distinguish these mechanisms, and to verify the suggested non-hysteretical mechanism experimentally? The answer is not evident at first glance, since by choosing appropriately parameters of a hysteretic curve, it is often possible to fit experimental data on amplitude-dependent variations in absorption and elasticity with a reasonable accuracy. Therefore, to address the question it is necessary to compare cases for which these mechanisms give essentially different predictions.

Note that the above conclusion on the close similarity of manifestations of both mechanisms was in fact obtained only for the case of self-action of a wave, that is, when a wave changes its own losses and velocity. However, as it is clear from the above consideration, the non-hysteretical mechanism should change the elastic and dissipative material properties not only for the wave itself, but also for other waves with different frequencies. For example, the non-hysteretical mechanism readily allows for estimating the influence of a stronger ("pump", using the terminology of nonlinear optics) wave $\sigma_p = \sigma_0 \cos(\omega_0 t)$ or $\varepsilon_p = \varepsilon_0 \cos(\omega_0 t)$ on another weaker probe wave ($\sigma_w = \tilde{\sigma}_0 \cos(\tilde{\omega}t)$ or $\varepsilon_w = \tilde{\varepsilon}_0 \cos(\tilde{\omega}t)$), for which $\tilde{\varepsilon} \ll \varepsilon_0$ and $\tilde{\omega} \neq \omega_0$. The pump wave should change both the mean velocity and the losses for the weak probe wave, and these changes produced by the stronger wave can be considered as given. Therefore, the effective density of the defects can be considered as a function of the pump wave amplitude ($\langle N \rangle = N(\varepsilon_0)$). Then the mean change both in the elastic moduli and in the decrements for the probe wave can be consistently evaluated using equations (8) through (10) and (21), (22).

Now let us discuss whether it is possible to separate this type of the sound-by-sound attenuation from conventional hysteretical losses, that is to eliminate for the probe wave the influence of losses connected to the hysteresis loops. In fact, the method of such elimination of hysteresis is well known, and it was used long ago in mechanics of high-precision measurement devices containing pendulum-like sensitive compo-

nents mounted on shafts. There was a problem how to avoid the frictional stick hysteresis in the dependence between the tilt angle of the pendulum and the applied force. Conventional liquid lubrication could not help, because in the initial state the pendulum had to be motionless, but the liquid lubrication could prevent stick only when the contacting surfaces have high enough relative velocity [49]. An alternative effective solution of the problem was based of the use of rapidly (either uniformly or oscillatory) rotating shaft of the pendulum, which provided high relative velocity at the interface of the solids and prevented the dry-friction stick and the corresponding hysteresis. Nowadays similar methods are widely spread not only in tribology to exclude frictional stick-slip phenomena [49], but in other applied problems in order to eliminate or to smooth influence of hysteretical, frictional and other nonlinearities (the so-called dither method) [50]. Physically both the adhesional and friction-stick hystereses originate due to the work necessary to break inter-atomic bonds. The macroscopical manifestation of these phenomena in a hysteresis curve is also similar in mechanical and acoustical problems. Therefore, the same method may be applied for our purpose to eliminate the influence of hysteretical losses for the weak probe wave (oscillation) by means of exciting in the medium an additional (pump) wave whose deformation rate is much higher than that in the probe wave. Due to this additional high-rate deformation the hysteretical losses will be eliminated for the weak probe wave, but certainly they will occur for the pump wave itself.

In the discussed case, this method has a clear macroscopic interpretation which does not depend neither on atomic origin of the hysteresis, nor on macroscopic form of the hysteresis curve. Indeed, in order to make the hysteretical losses manifest themselves, it is necessary to provide reverse movement of the point of state of the medium along the hysteretic loop on the "stress-strain" plane. This means that the strain rate in the probe wave must be large enough to produce such a reverse movement of the state point, thus producing hysteretical losses for this wave. In such a case, the area of the hysteretical loops (that is the losses) of the probe wave may be influenced by an additional stress field (the pump wave). On the stress-strain plane, this case may be imagined, for example, as a big hysteresis loop produced by a strong pump wave and a number of small loops produced by the higher-frequency probe wave, these smaller loops being embedded in the big loop. However, if the velocity of strain variation in the pump excitation is much higher than that in the probe wave, there is no hysteretical reverse for the weak wave (smaller loops do not exist), and the influence of hysteretical losses is eliminated for such a weak probe wave. Certainly, the weak wave is affected by the pump excitation via the material nonlinearity, but the conventional hysteretical losses for the probe wave are eliminated. The latter case is just what is necessary in order to separate the influence of the hysteretical and the non-hysteretical amplitude-dependent losses. Namely, the same strong enough pump-wave will affect the attenuation of the weak probe wave via the suggested non-hysteretical mechanism and simultaneously will eliminate the hysteretical losses for the probe wave.

The requirement of strong enough velocity of strain changes in the pump wave in case of harmonical excitations is equivalent to the following condition in terms of wave frequencies and strain amplitudes:

$$\omega_0 \epsilon_0 \gg \bar{\omega} \bar{\epsilon}, \quad (29)$$

where $\bar{\omega}, \bar{\epsilon}$ refer to the probe- and ω_0, ϵ_0 refer to the pump-wave. This relation should be provided in experiments in order to exclude conventional hysteretic losses for the weak probe wave.

As another feature of the nonlinearity-induced change in the decrement for the probe wave caused by the non-hysteretical mechanism, it may be mentioned that the nonlinear decrement should not display significant dependence on the probe wave frequency if the defects are significantly distributed over their elastic parameters (see equation (14) and the discussion of equations (17), (18) and Figure 3). This prediction may be readily verified experimentally (see the next section). Actually this consequence is the same as for the linear decrement, because in the discussed "cascade" mechanism (nonlinear elasticity + viscous losses = amplitude-dependent attenuation) physical origin of energy dissipation is the same as for the case of the linear attenuation. Due to common origin with linear attenuation, other features of the amplitude-dependent part of the decrement may be readily analyzed using equations (8) through (22) for the complementary amplitude-dependent losses and the elasticity changes. For example, the dependence of these effects on the type of the wave (longitudinal, shear) are readily inferred (see examples presented in Figure 4).

Therefore, despite certain resemblance, important differences between the non-hysteretical and hysteretical amplitude-dependent losses can be pointed out, which allow for separation of these mechanisms and experimental verification of the predicted features.

6. Comparison with the experimental data related to the suggested mechanism of amplitude-dependent losses

In this section we start from examples of known [27–29] experimental observations which cannot be explained in the framework of the hysteretical mechanism of amplitude-dependent attenuation, but which may be readily accounted for in the framework of the proposed non-hysteretical mechanism. In addition, original experimental demonstrations are presented. In all of these experiments, resonant longitudinal vibrations at lower modes were excited in rod resonators with one free and the other rigidly fixed boundary. In certain cases, additional high-frequency weak ultrasonic pulses were emitted to observe the influence of the stronger resonant excitation. The rods were cut from several kinds of rocks or from annealed copper which are typical microinhomogeneous materials and exhibit pronounced amplitude-dependent variations both in elasticity and in losses [5, 7, 27–32]. Let us briefly discuss these data from the point of

view of the formulated mechanism before turning to our experimental demonstration.

Note that effects of wave self-action, such as the nonlinear shift of the rod resonance frequencies, amplitude-dependent losses for the same resonance vibration, and generation of higher harmonics, conventionally were interpreted using phenomenological hysteretical models [5, 7, 13, 31] of piece-wise parabolic type. This approach provided reasonable qualitative description of each concrete effect, and gave agreement within 20–50% between the model parameters inferred from different effects. Analogous results on application of other approximations of hysteretical curves to description of the rod-resonant self-action effects were reported in review [18] (see also references herein).

In the other series of experiments with the same materials, effects of sound by sound attenuation were investigated for waves with significantly different amplitudes and frequencies. In particular, damping of pulsed high-frequency probe signals (several hundreds of kHz) under the action of an intensive $\epsilon_0 = 10^{-6} \dots 10^{-5}$ resonant vibration at several kHz was investigated [27–29]. The pulses propagated twice the rod length (forth and back) and demonstrated pronounced (up to 3 times) decrease in amplitude when the other strong harmonical wave was excited at lower rod resonances [27–29]. However, within the measurement accuracy (about several percents) there was no apparent change in the pulse propagation time in contrast to the easily observed nonlinear attenuation. That is, in these cases the material nonlinearity looked "purely dissipative". From the point of view of the discussion in the previous section, the conditions of elimination of hysteretical losses for the weak probe pulses were perfectly fulfilled in [27–29, 51]. The ratio of the amplitudes of the weak pulses and the strong pump vibration $\epsilon_0 / \bar{\epsilon}$ reached $10^3 \dots 10^4$, whereas the ratio of frequencies of the pulse carrier wave and the pump wave $\bar{\omega} / \omega_0$ was only 40...70 times. Therefore, the amplitude of the velocity of strain variations in the weak pulse was definitely much less ($10^1 \dots 10^3$ times) than in the pump wave (see equation 29), and, thus, not depending on a particular model of the material hysteresis, the influence of hysteretical losses for the weak wave was eliminated with high accuracy. Nevertheless, the dependence of the pulse attenuation on the pump wave amplitude was very pronounced, and since it could not be attributed to the influence of the hysteretical losses, it was supposed that the material exhibits another mechanism of amplitude-dependent attenuation [27]. To phenomenologically account for the observed nonlinear attenuation, amplitude-dependent viscous terms were added [27–32] to the equation of the material state, which allowed for fair matching the experimental data. The decrease in the probe wave amplitude may be readily described, whereas the nonlinear dissipative terms do not influence the wave velocity. Probably in some cases such "purely dissipative" nonlinearity may really occur due to non-viscous friction in the defects, but this require higher pump amplitudes, as it was argued in Section 4. On the other hand, the same materials exhibited strong odd-type nonlinear elasticity, since pronounced nonlinear shift of the resonance frequency occurred in the resonators at excitation amplitudes

$\varepsilon_0 = 10^{-6} \dots 10^{-5}$. Therefore, the conditions for manifestation of the amplitude-dependent attenuation described in Sections 4,5 were provided.

Now we shall make some estimates which can be applied to the discussed measurements and which elucidate why the complementary variation in the pulse delay apparently was not mentioned in [27–29], although the above suggested model predicts both the delay and attenuation for the probe wave. Let us suppose the following experimental parameters, which are comparable to those reported in [27–29]. Let take the sound velocity $c = 3600$ m/s for the rod (Young) wave; the carrier frequency of the probe pulse $f = 200$ kHz; the corresponding wavelength $\lambda = c/f \approx 1.8$ cm; the rod length $L \approx 30$ cm. Then the pulse propagation time T forth and back along the rod is $T = 2L/c \approx 170$ μ s. For a thin rod with one free and one rigid boundary, the modal shapes have the normalized forms $\varphi(x) = (2/L) \sin(\pi(n - 1/2)x/L)$, $n = 1, 2 \dots$ [7], and, for example, the first quater wavelength resonance has frequency $F_1 = c/(4L) \approx 3$ kHz. Experiments indicate that in the discussed amplitude range, the nonlinear shift of the resonance frequency normally is linearly proportional to the strain amplitude ε_0 , that is $\delta F(\varepsilon_0)/F_n \propto \varepsilon_0$ [5, 7, 18], and, therefore, the averaged variation in the local sound speed is also linearly dependent on the local strain amplitude, $\delta c(\varepsilon_0(x))/c \propto \varepsilon_0(x)$. For example, for the lowest mode $\varepsilon_0(x) \propto \varphi_1(x) \propto \sin(\pi x/2L)$. Conventional procedures of the perturbation theory yield for the resonance frequency shift $\delta F_n(\varepsilon_0)/F_n$ and for the perturbation of the pulse propagation time $\delta T(\varepsilon_0)/T$:

$$\begin{aligned} \delta F_n(\varepsilon_0)/F_n &= - \int_0^L \frac{\delta c[\varepsilon_0(x)]}{c} \varphi_n^2(x) dx, \\ \delta T(\varepsilon_0)/T &= - \int_0^L \frac{\delta c[\varepsilon_0(x)]}{c} dx, \end{aligned} \quad (30)$$

therefore, in the considered case $\delta T(\varepsilon_0)/T = (3/4) \delta F_n(\varepsilon_0)/F_n$, that is the relative variation in the pulse delay time is 4/3 times smaller than for the resonance frequency. For the pump amplitudes $\varepsilon_0 = 10^{-6} \dots 10^{-5}$, the typical magnitude of the resonance shift is $\delta F_n(\varepsilon_0)/F_n = 10^{-2}$, which, according to (30), corresponds to the twice as big time-averaged variation of the sound speed $\delta c(\varepsilon_0)/c = (2\pi/3)\delta F_n(\varepsilon_0)/F_n \approx 2 \cdot 10^{-2}$ in the pump-mode maximum. The corresponding time-delay for the probe wave is $\delta T(\varepsilon_0) \approx (3/4) \cdot 10^{-2} \cdot 170 \mu\text{s} \approx 1.3 \mu\text{s}$, which is much less than the duration of the pulse containing several carrier-wave periods, and is only about 1/4 of the period $1/f = 1/200$ kHz = 5 μs of the carrier wave. Such a small averaged delay can be reliably noticed only when the pulse envelope is synchronized with the carrier, and, therefore, coherent signal accumulation is possible. In experiments [27–29] these conditions were not provided, the delay measurement inaccuracy was 4 ... 5 μs , which explains why the pulse shift was not observed.

We reproduced the discussed above experimental conditions, but provided the synchronization of the pulse envelope and the carrier wave and the possibility of signal accumulation by a digital oscilloscope. The experiment confirmed

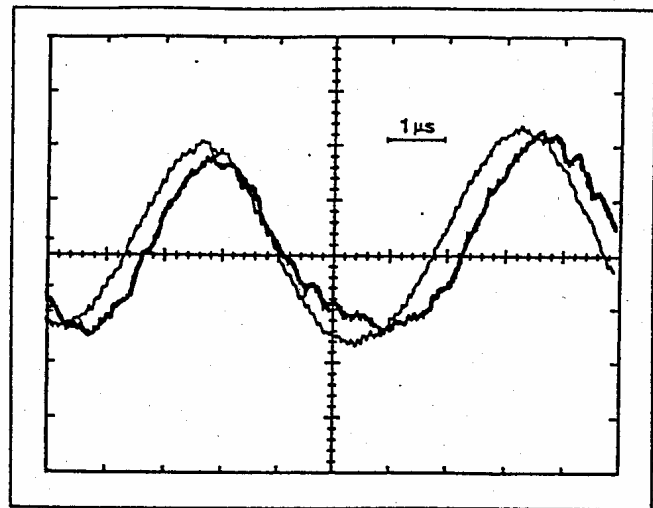


Figure 5. Examples of normalized records of the central parts of the probe pulses. The thin line is the reference signal in the absence of the pump wave; the thick line is the delayed and attenuated signal in the presence of the pump wave. The amplification of the delayed probe wave is 2.5 times larger than that of the reference signal. Both records are accumulated over 32 shots.

that in the pulse envelope the nonlinearity-induced shift is impossible to notice, but in the carrier wave the delay is quite noticeable if coherent signal accumulation is used. An example of such a record of the simultaneously displayed fragments of the reference pulse (thin line) without the pump wave and the delayed signal (thick line) is presented in Figure 5. The strong pump-signal was filtered out by a high-pass filter which provided >80 dB signal reduction at the pump frequency. For convenience, both signals in the record are normalized to approximately the same amplitude, using 2.5 times smaller amplification for the reference pulse in order to compensate the nonlinearity-induced attenuation of the delayed pulse. Using the record, the delay may be estimated as $\langle \delta T_{\text{exp.}} \rangle \approx 0.4 \dots 0.5 \mu\text{s}$. The corresponding decrease in the resonance frequency for the pump wave (the first resonance at $F_1 = 3139$ Hz) was $\delta F_1(\varepsilon_0) = 28$ Hz, or $\delta F_n(\varepsilon_0)/F_n = 9 \cdot 10^{-3}$ at strain amplitude $\varepsilon_0 \approx 8 \cdot 10^{-6}$. At first glance, the above estimate based on equation (30) for the time-averaged perturbation $\delta T(\varepsilon_0(x))$ apparently yields 2.5–3 times larger value of 1.3 μs . However, in fact the delay displayed at the oscilloscope record is somewhat different than the estimate based on equations (30). The digital oscilloscope does not average the magnitudes of the individual pulse delays δT , as is supposed in equation (30), but *accumulates the pulses* which has different delays and different magnitudes of the non-linear attenuation. Indeed, since the time of pulse propagation forth and back was equal to 1/2 period of the pump wave, the distribution $\delta c(\varepsilon_0(x))$ (averaged over the carrier period) was "breathing" during the pulse propagation, and also randomly varied between different pulses, because the pump-frequency was not synchronized with the pulse-repetition frequency. The pulses, which were less attenuated, simultaneously had smaller delays and vice versa. Therefore, both the resultant amplitude and the delay of the accumulated pulse were mainly determined by

the pulses with *larger* amplitudes and *smaller* delays. The 3 times difference in the amplitudes between the individual pulses readily accounts for the apparent 2.5–3 times discrepancy between the estimate (30) and the smaller experimental "averaged" delay displayed in Figure 5.

Figure 6 displays with 50 times smaller resolution examples of the single-shot records of the emitted and the received probe pulses. Comparison of the pulse amplitudes without the pump wave (Figure 6a) and the nonlinearly attenuated pulse (Figure 6b) illustrates that attenuation of some pulses was significantly larger than the averaged value of 2.5 times; and even for a given pulse different parts of its envelope exhibited significantly different attenuation, since the pump-wave phase changed significantly within the pulse duration. The difference in the attenuation either between different pulses or even between the parts of the same pulse was more than 3 times, which reduced several times the apparent "average" delay in comparison with the "true" averaging of the individual delays in equation (30). Therefore, actually the magnitudes of the experimentally observed probe pulse shift and the resonance-shift for the pump wave agree well with the theoretical prediction based on the averaged nonlinear variation in the Young modulus.

Now let us compare the value of the expected and the experimentally observed attenuation complementary to such a variation in the elastic modulus. According to the examples of the calculations presented in Figure 4(a) for the Young wave, the corresponding change in the averaged decrement (both for the pump and for the weaker probe waves) should be of the same magnitude. In case of about 1% shift of the resonance frequency $\delta F_n(\epsilon_0)/F_n$ the complementary averaged increase in the decrement $\delta\theta(\epsilon_0) \approx \delta c/c = (2\pi/3)\delta F_n/F_n \approx 2 \cdot 10^{-2}$.

For simplicity, first we neglect the inhomogeneous distribution of the pump wave amplitude along the rod. Then the increase in the decrement $\delta\theta(\epsilon_0) \approx 2 \cdot 10^{-2}$ together with the non-dimensional propagation length $2L/\lambda \approx 33$ yield the decrease in the probe wave amplitude by the factor of

$$\bar{\epsilon}(\epsilon_0 = 0)/\bar{\epsilon}(\epsilon_0) \approx \exp[\delta\theta(\epsilon_0)2L/\lambda] \approx 2. \quad (31)$$

This simplified estimate agree fairly well with both our observations and typical amplitude variations reported in experiments [25–27]. For more detailed comparison the method of the averaging must be considered more attentively like in the above case. Namely, expressions (17)–(22) were obtained for the time-averaged local magnitude of the decrement in the material $\delta\theta(\epsilon_0) = \langle \delta\theta \rangle$. However, when the attenuation in the experiment is estimated by measuring the accumulated decrease in the amplitudes of the pulses, actually the factor $\exp[\int \delta\theta dx/\lambda]$ rather than $\delta\theta$ is averaged for a number of different pulses, and along the rod length for each pulse. In the discussed experiment the argument $\alpha = \int \delta\theta dx/\lambda$ of the exponent (31) varied strongly for different pulses, from magnitudes much less than unity up to several units. Therefore, the averaged factor $\langle \exp[\int \delta\theta dx/\lambda] \rangle$ in such a case is noticeably greater than $\exp[\langle \int \delta\theta dx/\lambda \rangle]$ because of the influence of the rapid exponential function on the result of

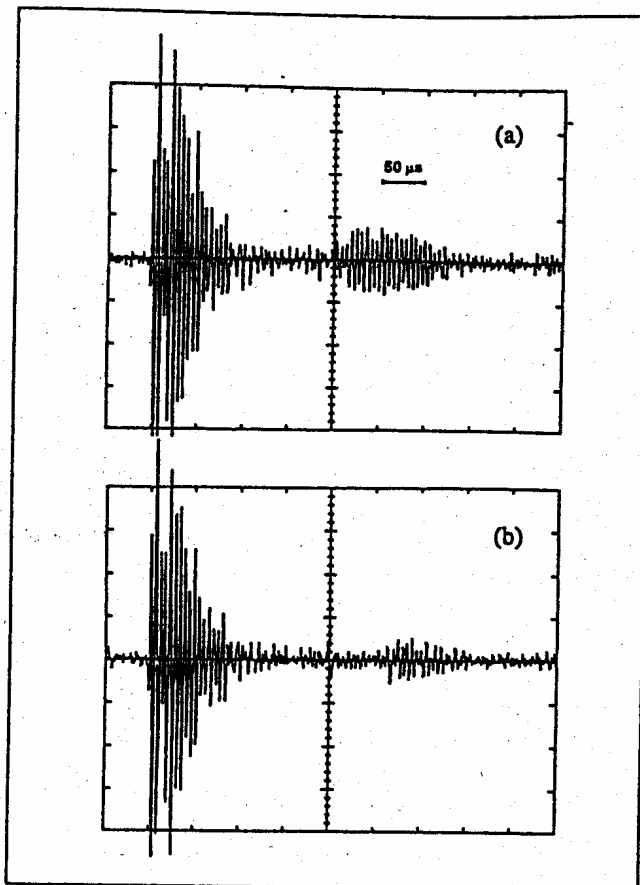


Figure 6. Examples of single shot records of the emitted pulse (the left part of the records) and the pulse propagated twice along the rod (the right part of the records). (a) - the record in the absence of the pump wave showing the reference form of the propagated pulse; (b) - the nonlinearity-attenuated probe pulse at the same pump level as for the time-averaged record presented in Figure 5 displaying the central fragment of the pulse. The non-uniform attenuation within the pulse duration is clearly seen in the record (b): the leading half of the pulse is attenuated down to the noise level, whereas the rear part of the pulse is only slightly attenuated.

the averaging. For example, the difference $\alpha_1 = 0.1$ and $\alpha_2 = 1.3$ between the pulses yields for the averaged value $\langle \alpha \rangle$ the attenuation factor $\exp[\langle \alpha \rangle] \approx 2.0$, whereas the averaging of the whole attenuation factor yields noticeably larger value $\langle \exp[\alpha] \rangle \approx 2.4$. Thus, accumulation of the randomly attenuated pulses results in the apparently stronger attenuation and apparently smaller delay as it was elucidated above. Therefore, the experimental ratio between the nonlinear attenuation/delay of the probe pulse is in a good agreement with the prediction based on the suggested mechanism.

For the completeness of the above experiment discussion, we may add that the non-local scattering mechanism [41] of the weak/strong wave interaction is unlikely to account for the observed 2–3 times average attenuation of the probe signal and even stronger attenuation at certain single shots. A simple estimate of the magnitude of scattering expected for the experimental magnitude of the nonlinear variation in the sound velocity $\delta c/c \sim 10^{-2}$ shows that in order to change the probe-wave amplitude 2–3 times, there must be synchronous accumulation of 200–300 individual acts of

scattering. Since the interaction length in our experiment was about 30 lengths of the probe wave and only 1/2 wave length of the pump wave, these conditions were not fulfilled, though in other cases the scattering mechanism may significantly affect results of wave interactions and should be taken into account.

Summarizing the performed estimates, we may conclude that the proposed mechanism of the amplitude-dependent attenuation suggests a plausible explanation for the effect of strong attenuation of weak pulses under the action of a strong pump excitation, which could not be attributed to hysteretical losses. These effects illustrate that at certain conditions the microstructure-induced amplitude-dependent attenuation can be much more pronounced compared to the complementary time-delay variations and similar nonlinear-elastic effects. It is important to note that this difference becomes stronger at larger propagation distances. Indeed, the time delay (of phase shift) accumulates linearly proportional to the propagation distance, whereas the wave attenuation (of any origin) is exponentially proportional to the distance L/λ (see equation 31). Therefore, at large distances $L/\lambda \ll 1$, the nonlinearity-produced variation in the wave amplitude can be significantly larger compared to the variation in the propagation time. Apparently the material properties in such cases may produce at first glance an impression of "purely dissipative nonlinearity" like in the above example and experiments [27–29]. Here we restrict ourselves to the performed above estimates relevant to the pulse-resonant interactions. More detailed comparison requires correspondingly more detailed modelling of properties of both the individual defects and the density of distribution over the parameters of the defects.

A few more general, but important conclusions allowing for experimental verification may be additionally inferred from the close similarity of properties of the linear and the nonlinear microstructure-induced perturbations in the elasticity and the decrements in microinhomogeneous solids. In particular, since equations (8)–(10) and (21), (22) indicate that nonlinear variations both in the elastic moduli and in the decrements are determined mainly by the amplitude dependence of the effective defects density $N = N(\varepsilon_0)$, then, consequently, the amplitude dependencies of $\delta\theta(\varepsilon_0)$ and $\delta c(\varepsilon_0)$ must be similar both for static and for period-averaged variations (see also the discussion of the estimates presented in Figure 4). Available experimental data, indeed, satisfactory agree with this conclusion. For example, dependencies of the attenuation and the modulus on static pressure [24] exhibit such a close functional resemblance and the variation magnitudes agree well with the model predictions.

In case of wave self-action, resonant experiments [7] and other similar measurements by Nazarov [42] or an independent example presented in [21, p.169] and obtained by Winkler [43] also exhibit the similar amplitude behavior of the elasticity and the attenuation. However, unlike the case of the static pressure effect, the data on self-action of oscillatory excitations are not transparent enough for rigorous comparison with the discussed model, because in this case both the non-hysteretical and conventional hysteretical amplitude-dependent dissipation may occur simultaneously.

Let us also address briefly the expected dependence of the nonlinear parameter variations on the pump excitation frequency. Generally speaking, the nonlinear change in the effective defect density $\Delta N(\varepsilon_0)$ can depend not only on the strain amplitude ε_0 , but also on amplitude $\omega\varepsilon_0$ of the strain rate, because the defects evidently exhibit relaxation properties (see equations (3), (4) in which the corresponding viscous-like terms are introduced). That is the dispersion of the nonlinear variations, which is of the same origin as for the linear elasticity and attenuation, must occur in the material. Rigorous prediction of frequency dependence $\Delta N(\omega_0, \varepsilon_0)$ requires consideration of concrete nonlinear models of defect dynamics under oscillatory stress action and in the considered case it may be analyzed like in 1D paper [53]. Qualitatively it may be argued that the dispersion of the nonlinearity in a material with a wide relaxation spectrum of the defects must be weak due to the smoothing of the relaxation peaks over the relaxation spectrum much like in the linear case, in which the weak logarithmic dispersion of the sound velocity occurs [38–40]. More careful analysis of this question is beyond the scope of the present paper. However, in this context we may mention experiments [54] in which at the variation in the pump frequency ω_0 by the order of magnitude, the nonlinearity-induced losses of the high-frequency probe wave varied only within 10–50 percents. Using the same analogy with the linear case, weak dependence of the nonlinear decrement on the probe wave frequency may be also predicted. The corresponding effect observation at 60-times lower signal frequency than in the above pulse-resonant experiment is described below.

This experimental demonstration of the nonlinearity-induced losses of the non-hysteretical origin has the following goals. The first goal is to give an example of the nonlinear attenuation of a probe wave, whose frequency $\bar{\omega}$ is significantly (3 times) lower than that (ω_0) of the pump-wave, unlike the previous examples in which $\bar{\omega} \sim (60 \dots 70)\omega_0$. Thus the elimination of the hysteretical losses for the weak low-frequency wave due to a strong higher-frequency action is more close to the classical method of dithering [49, 50] than in the above discussed pulse-resonant case of $\bar{\omega} \gg \omega_0$. The second goal is to experimentally demonstrate the effect of the nonlinear dissipation in a more pure form. Namely, the case will be demonstrated, in which the probe signal attenuation is proportional to the decrement variation $\delta\theta(\varepsilon_0) \ll 1$, whereas the influence of the complementary variation in the elasticity is reduced down to the second-order ($[\delta c(\varepsilon_0)/c]^2 \sim [\delta\theta(\varepsilon_0)]^2 \ll \delta\theta(\varepsilon_0)$) correction to the probe-signal amplitude. This difference is achieved due to special choice of parameters of the waves. Note for comparison that in the discussed above pulse-resonant experiments, both the delay and the attenuation of the probe pulse were determined by the first-order nonlinear variations $\delta c(\varepsilon_0)/c \sim \delta\theta(\varepsilon_0)$.

To observe the "pure" effect we excited the pump-oscillation at the second resonance of the described above rod-resonator. The probe wave was lower in frequency. At first glance it seems convenient to choose the probe wave frequency away from resonances. However, in a relatively

high-quality resonator (the Q-factor was about 200 for 5 lower modes of the copper rod), the amplitude of an oscillation excited out of a resonance practically does not depend on the losses in the resonator, and is almost entirely determined by the frequency de-tuning from the resonance. On the other hand, near a resonance, the oscillation amplitude is determined by variations both in the resonance frequency shift and the material decrement, whereas our goal is to single out these effects. Nevertheless, it is possible to separate the influence of the nonlinear variation $\delta\theta_n^{\text{probe}}(\varepsilon_0)$ in the material decrement, and to effectively eliminate the influence of the complementary variation in the resonance frequency. This may be achieved if the probe wave frequency is initially tuned *exactly* to the resonance maximum F_n , and the nonlinear variation $\delta F_n^{\text{probe}}(\varepsilon_0)$ in the resonance frequency for the probe-signal is small compared to the width $\Delta F_n^{\text{res.}}$ of the resonance curve:

$$\delta F_n^{\text{probe}}(\varepsilon_0)/F_n \sim \delta\theta_n^{\text{probe}}(\varepsilon_0) \ll \Delta F_n^{\text{res.}}/F_n. \quad (32)$$

Indeed, it is well known that due to the zero slope of the tangent at the resonance maximum, a small shift from the resonance frequency, $\delta F_n^{\text{probe}}(\varepsilon_0)/\Delta F_n^{\text{res.}} \ll 1$, affects the signal amplitude only in the *second order* of the frequency shift magnitude. On the other hand, the variation in the decrement $\delta\theta_n^{\text{probe}}(\varepsilon_0) \sim \delta F_n^{\text{probe}}(\varepsilon_0)/F_n$ influences the resonant signal amplitude in the *first order* of its magnitude. However, if the resonance frequency shift further increases and becomes comparable with the width of the resonance, $\delta F_n^{\text{probe}}(\varepsilon_0)/F_n \sim \delta\theta_n^{\text{probe}}(\varepsilon_0) \sim \Delta F_n^{\text{res.}}/F_n$, then both complementary variations in the elastic $\delta F_n^{\text{probe}}/F_n$ and dissipative $\delta\theta_n^{\text{probe}}$ properties influence the probe signal amplitude in the same order of magnitude, and the action of such strong variations cannot be discriminated.

The above arguments show that the use of a moderate pump-wave amplitude, for which conditions (29) and (32) are simultaneously fulfilled, eliminates for the probe wave the influence of hysteretical losses together with the influence of the resonance shift caused by the pump wave. This allows us to reach the stated goal: to observe the non-hysteretical amplitude-dependent attenuation of the probe wave in the desired "pure" form. However, the effect must be inevitably limited to a small relative variation in the signal amplitude, as it is elucidated above.

In the experiment, the pump wave was excited at frequency $F_1 = 10120$ Hz of the second rod-resonance, and the probe one was tuned to the lowest first resonance at 3378 Hz. Initial (small-amplitude) quality factors for the first and the second resonances were $F_1/\Delta F_1^{\text{res.}} = Q_1 \approx 230$ and $F_2/\Delta F_2^{\text{res.}} = Q_2 \approx 180$, correspondingly (the resonance curve widths were $\Delta F_1^{\text{res.}} \approx 14.5$ Hz and $\Delta F_2^{\text{res.}} \approx 55$ Hz). For the pump amplitudes ε_0 between 10^{-6} and 10^{-5} , the nonlinear frequency shift was still too high $\delta F_1(\varepsilon_0)/F_1 \approx 10^{-2}$, which was larger than the initial width of the resonances $F_{1,2}^{\text{res.}}/\Delta F_1 \approx (4 \dots 5) \cdot 10^{-3}$. Therefore, following the above conclusions, in order to single out the effect of the nonlinear attenuation, we used smaller pump levels ($\varepsilon_0 \approx 1 \dots 2 \cdot 10^{-7}$), for which the nonlinear correction of the decrement $\delta\theta_1(\varepsilon_0)/\theta_1$ measured for the pump wave was

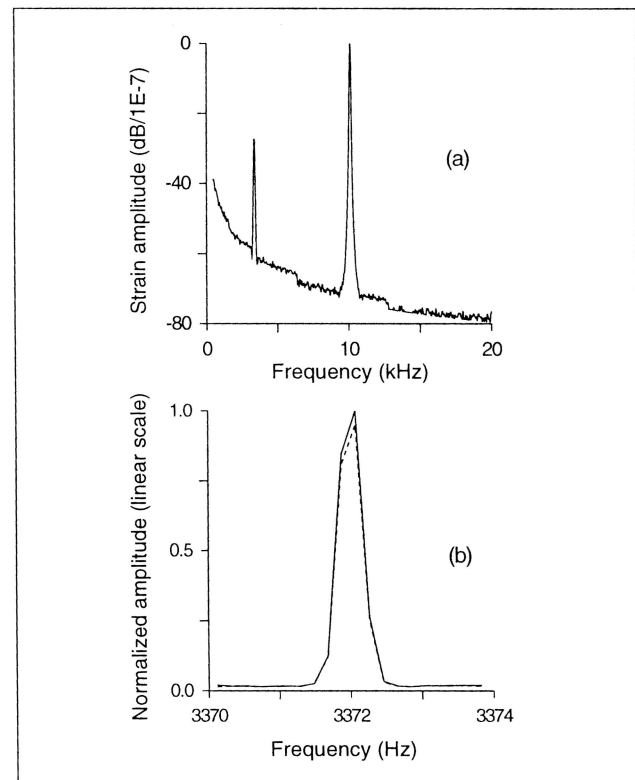


Figure 7. A "pure" experimental example of the suppression of the probe wave under the action of the pump wave due to the dissipative nonlinearity of the material. Both the influence of the resonance frequency shift due to the elastic nonlinearity and conventional hysteretical losses are negligible due to the appropriate choice of the pump- and the probe-wave amplitudes. (a) – the spectrum at the bi-harmonical excitation, the probe signal being tuned to the 1-resonance, and the pump being tuned to the 2-nd resonance at 3-times higher frequency; (b) – the spectral zoom for the low-frequency probe wave without the pump (the solid line) and in the presence of the high-frequency pump (the dashed line).

only about 3–5 percent, and the ratio $\delta F_{1,2}(\varepsilon_0)/\Delta F_{1,2}^{\text{res.}}$ was of the same order of magnitude.

In these conditions, the variation in the probe wave amplitude due to the nonlinear variation in the decrement is proportional to $\delta\theta_1(\varepsilon_0)/\theta_1 \ll 1$ (about $4 \cdot 10^{-2}$) whereas, the effect due to the resonance shift gives a negligible higher-order ($O(\cdot 10^{-3})$) correction. Thus occurrence of the decrease in the probe wave amplitude at the chosen small enough pump level is almost entirely due to the nonlinear variation in the dissipation. The corresponding example of experimental records is presented in Figure 7. Figure 7a demonstrates relative level of strain in the probe and in the pump waves (the difference between the strain rates was 3 times larger due to the 3 times difference in the frequencies). Therefore, condition (29) of elimination of hysteretical losses for the probe wave was well satisfied. The next Figure 7b shows the decrease in the amplitude of the probe wave of about 4% (or 0.4 dB) when the pump is switched on. This difference agree well with the magnitude of the resonance-frequency variation, and is much higher than the measurement inaccuracy, since due to signal filtration and accumulation the measurement results were reproducible within 0.02 dB.

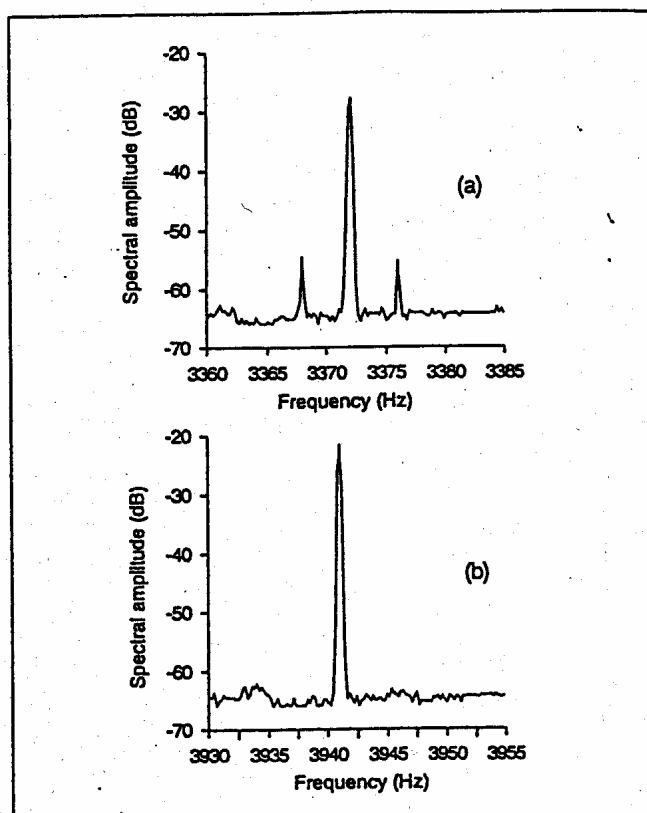


Figure 8. An example of the modulation spectrum obtained in the microinhomogeneous copper rod (a) and the similar spectrum without signs of modulation obtained at similar conditions in the reference homogeneous rod made of glass (b).

We stress once again that in the last example the effect strength was intentionally limited in order to obtain the manifestation of the amplitude-dependent losses in the most pure form, and to eliminate the influence of the nonlinear shift of the resonance on the probe wave amplitude. The observed amplitude decrease, therefore, could not be attributed to hysteretical losses of the probe signal, since the strain rate in the pump wave was high enough to eliminate hysteretical loops for the weak probe wave. On the other hand, the suggested non-hysteretical mechanism readily accounts for the phenomenon and fairly well predicts the value of the ratio between the observed complementary nonlinear variations in the losses $\delta\theta^{\text{probe}}(\epsilon_0)$ and the elasticity $\delta F_{1,2}(\epsilon_0)/F_{1,2}$.

Note finally, that the considered method of the effect observation has only an academic interest, since it requires too many experimental precautions. As another interesting and practically more convenient possibility to observe the nonlinearity-produced changes in the probe signal, the usage of a modulated pump wave can be suggested. In this case, due to the dependence of the material properties on the amplitude of the modulated the pump wave, the probe wave should also acquire a modulation. To demonstrate the effect, we used the same frequencies and amplitudes of the probe and the pump waves as in Figure 7a, but unlike the previous case the pump wave had sinusoidal amplitude modulation at low frequency 4 Hz with 100% modulation depth. This caused the corresponding slow modulation of the material

properties and resulted in the modulation of the probe wave. An example of its modulation spectrum is given in Figure 8a. The modulation side-lobes of the probe wave are clearly seen even though we intentionally used a rather weak pump level, which proves the high sensitivity of the effect. The level of the sidelobes is about -28 ± 1 dB (that is about 4% of the central line amplitude), and agree well with the magnitude of the static decrease in the probe wave amplitude shown in Figure 7b. For comparison, another spectrum obtained for a reference rod made of glass (a homogeneous material with weak atomic nonlinearity) is presented in Figure 8b and displays no sign of such a modulation. Note, that similar nonlinear-modulation effects were previously observed in defect-containing solid samples using directly low frequency pump-vibrations (at frequency from several Hertz to several tens of Hertz) [55–57]. However, often the excitation of a relatively intensive vibration at such a low frequency is a difficult technical problem, so the use of the modulated high frequency pump wave can be more advantageous in diagnostical applications. The effect of the amplitude-dependent attenuation does not require spatial synchronism and can be observed both for co-propagating and counter-propagating waves. When the interaction length is large enough, the resultant amplitude modulation can be rather strong even at small variation in the decrement, which seems to be very promising for practical nonlinear methods of acoustic and seismic diagnostics.

7. Conclusion

The consideration of nonlinear effects in microinhomogeneous solids presented in this paper demonstrates that, although the phenomena originate from the same microstructural material features, in general, the character of the nonlinear effects can be formed by several different mechanisms of the nonlinearity manifestation. In this paper we focused on the nonlinear (amplitude-dependent) variation in local attenuation in microinhomogeneous materials, and suggested a new mechanism of this phenomenon. Unlike other models of the amplitude-dependent attenuation this mechanism requires neither conventional hysteretical losses, nor frictional (non-viscous) dissipation at the defects. The key points of this mechanism are (i) conventional viscous-like (e.g. thermal) losses at the defects and (ii) nonlinearity of defects' elastic parameters. Combined influence of these two factors results in occurrence of macroscopic amplitude-dependent attenuation in the material. In particular, hysteretical nonlinearity of the defects may also manifest itself via this mechanism in addition to the conventional hysteretical losses described by the area of the hysteresis loop.

At certain conditions and for particular effects, one of the mechanisms can dominate whereas in other cases contributions of different mechanisms could be comparable resulting in a rather complex character of functional dependencies of the effects. For example, at self-action of intensive waves, the contributions of conventional hysteretical and the suggested non-hysteretical amplitude-dependent losses can be comparable. In other cases, for example, in nonlinear variation of

attenuation of a weak probe wave under the action of another stronger wave, or in case of influence of quasistatic loading, the proposed new mechanism can dominate.

The predictions of the proposed mechanism are in a fair agreement with the own experiments and published experimental data. In particular, an explanation is proposed for experimental observations of strong dissipative nonlinearity [27–29], which could not be explained by hysteretical losses and required to introduce phenomenological nonlinear-dissipative terms into equation of state of microinhomogeneous solids.

Generically, the results of this paper are based on the same approach which in a series of papers (e.g. [34–40, 53]) was developed to account for a wide variety of acoustical features of microinhomogeneous solids: near-constant quality factor and the complementary dispersion, anomalous high level of elastic nonlinearity, dispersion of nonlinear parameters and, in the present paper, the amplitude-dependent attenuation. The modeling of the material properties in this approach may be characterized as micromechanical description, in which the individual defects were described by phenomenological parameters (elastic moduli, effective viscous parameters, nonlinearity function). This combination of consistent micromechanical analysis and phenomenology in the defect description is a practically convenient way allowing for important predictions even without detailed physical models of the defects. If necessary, however, concrete defect models may be used to infer defect's parameters, which may be substituted in the suggested micromechanical material models, thus transforming them into consequent physical modeling of the material starting from the microdefect level.

The effects inferred from the suggested mechanism of the elasto-dissipative nonlinearity, therefore, agree well with the other models [34–40, 53] which consistently account for the wide variety of experimental data on the microstructure-induced linear and nonlinear elastic/dissipative properties of microinhomogeneous solids. The predicted amplitude-dependent dissipative effects are rather sensitive to the changes of material structure, which provides an additional argument in favor of high potential of exploitation of the nonlinear acoustic and seismic effects in diagnostical applications.

Acknowledgement

The work was supported by a grant of the Research Council of KU Leuven. Authors are grateful to Philips Components B.V. (The Netherlands) for supplying piezo-components and to Prof. M. Wevers from MTM Department of KU Leuven for providing the rod-samples used in the experiments. Reviewer's remarks were very useful for the improvement of the manuscript.

References

- [1] D. H. Johnston, M. N. Toksöz: Thermal cracking and amplitude dependent attenuation. *J. Geophys. Res.* 85 (1980) 937–942.
- [2] V. N. Bakulin, A. G. Protosenko: Nonlinear effects in travel of elastic waves through rocks. *Transl. USSR Acad. Sci. Earth Sci. Sect.* 263 (1981) 314–316.
- [3] A. V. Nikolaev, I. N. Galkin (eds.): *Problems of nonlinear seismics*. Nauka publishers, Moscow, 1987, (In Russian).
- [4] I. A. Beresnev, V. A. Nikolaev: Experimental investigations of nonlinear seismic effects. *Phys. of the Earth and Planetary Interiors* 50 (1988) 83–87.
- [5] V. E. Nazarov, L. A. Ostrovsky, I. A. Soustova, A. M. Sutin: Nonlinear acoustics of micro-inhomogeneous media. *Phys. of the Earth and Planetary Interiors* 50 (1988) 65–73.
- [6] L. A. Ostrovsky: On nonlinear acoustics of weakly-compressible media. *Akust. Zhurn.* 34 (1988) 908–913. [Engl. Transl.: Sov. Phys. Acoust. 34(3), (1988), 523–528].
- [7] V. E. Nazarov: Nonlinear acoustic effects in unannealed copper. *Akust. Zhurn.* 37 (1991) 150–156. [Engl. Transl. *Acoust. Phys.* 37(1), (1991)].
- [8] L. A. Ostrovsky: Wave processes in media with strong acoustic nonlinearity. *J. Acoust. Soc. Am.* 90 (1991) 3332–3337.
- [9] I. Y. Belyaeva, V. Y. Zaitsev, E. M. Timanin: Experimental study of nonlinear elastic properties of grainy media with non-ideal packing. *Acoust. Physics* 40 (1994) 789–793.
- [10] V. Y. Zaitsev: Nonideally packed granular media: Numerical modeling of elastic nonlinear properties. *Acoust. Physics* 41 (1995) 385–391.
- [11] P. A. Johnson, P. N. J. Rasolofosaon: Manifestation of nonlinear elasticity in rock: convincing evidence over large frequency and strain intervals from laboratory studies. *Nonlinear Processes in Geophysics* 3 (1996) 77–88.
- [12] V. E. Nazarov, A. M. Sutin: Nonlinear elastic constants of solids with cracks. *J. Acoust. Soc. Amer.* 102 (1997) 3349–3354.
- [13] K. Naugolnykh, L. Ostrovsky: *Nonlinear wave processes in acoustics*. Cambridge University Press, MA, USA, 1998.
- [14] V. Gusev, C. Glorieux, W. Lauriks, J. Thoen: Nonlinear bulk and surface shear acoustic waves in materials with hysteretic and endpoint memory. *Phys. Lett. A* 232 (1997) 77–86.
- [15] V. E. Gusev, W. Lauriks, J. Thoen: Dispersion of nonlinearity, nonlinear dispersion and absorption of sound in microinhomogeneous materials. *J. Acoust. Soc. Amer.* 103 (1998) 3216–3226.
- [16] A. N. Tutuncu, A. L. Podio, A. R. Gregory, M. M. Sharma: Nonlinear viscoelastic behavior of sedimentary rocks, Part I: Effect of frequency and strain amplitude. *Geophysics* 63 (1998) 184–194.
- [17] A. N. Tutuncu, A. L. Podio, M. M. Sharma: Nonlinear viscoelastic behavior of sedimentary rocks, Part II: Hysteresis effects and influence of type of fluid on elastic moduli. *Geophysics* 63 (1998) 195–203.
- [18] R. Guyer, P. Johnson: Nonlinear mesoscopic elasticity: Evidence for a new class of materials. *Physics Today*, April issue (1999) 30–36.
- [19] W. Mason (ed.): *Physical acoustics, principles and methods*. Vol.3, Pt.B, lattice dynamics. Academic Press, New York and London, 1965.
- [20] M. N. Toksöz, D. H. Johnston, A. Timur: Attenuation of seismic waves in dry and saturated rocks: I. Laboratory measurements. *Geophysics* 44 (1979) 681–690.
- [21] M. N. Toksöz, D. H. Johnston, A. Timur: Attenuation of seismic waves in dry and saturated rocks: II. Mechanisms. *Geophysics* 44 (1979) 691–711.
- [22] K. Aki, P. G. Richards: *Quantitative seismology*, Vol.1. W. H. Freeman and Company, San Francisco, 1980.
- [23] T. Bourbié, O. Coussy, B. Zinszner: *Acoustique des milieux poreux*, publications de l'institut français du pétrole. Editions Technique, Paris, 1986.
- [24] R. B. Gordon, L. A. Davis: Velocity and attenuation of seismic waves in imperfectly elastic rock. *J. Geophys. Res.* 73 (1968) 3917–3935.
- [25] G. Mavko: Frictional attenuation: an inherent amplitude dependence. *J. Geophys. Res.* 4 (1979) 4769–4775.
- [26] D. H. Johnston: Attenuation: a state of the art summary. – In: "Seismic wave attenuation" *Geophysics Reprint series* No.2.

Society of exploration geophysicists, Tulsa, OK, 1981, 123–135.

[27] V. E. Nazarov: Sound damping by sound in metals. *Acoustics Letters* 15 (1991) 22–25.

[28] V. E. Nazarov: Sound damping by sound in unannealed copper. *Akust. Zhurn.* 37 (1991) 825–826. [Engl. Transl.: Sov. Phys. Acoust. 37(4), (1991)].

[29] S. V. Zimenkov, V. E. Nazarov: Dissipative acoustic nonlinearity of copper. *Fizika Metallov i Metallovedenie* 3 (1992) 62–65. (in Russian) [Engl. Transl.: Physics of Metals and Metallography, No 3 (1992)].

[30] V. E. Nazarov, S. V. Zimenkov: Self-action of acoustic waves in rocks. *Acoustics Letters* 16 (1993) 198–201.

[31] S. V. Zimenkov, V. E. Nazarov: Nonlinear propagation of acoustic waves in rocks. *Fizika Zemli (Izv. Acad. Sci. USSR Phys. Solid Earth)* 5 (1994) 62–64. (in Russian).

[32] V. E. Nazarov: Self-action of elastic waves in media with dissipative nonlinearity. *Acoustics Letters* 17 (1994) 145–149.

[33] V. Y. Zaitsev, V. E. Nazarov: Elastic waves in media with nonlinear dissipation. *Akust. Zhurn.* 44 (1998) 362–368. [Engl. Transl.: Acoustical Physics, 44(3), (1998), 305–311].

[34] V. Y. Zaitsev: A model of anomalous acoustic nonlinearity of micro-inhomogeneous media. *Acoustics Letters* 19 (1996) 171–176.

[35] I. Y. Belyaeva, V. Y. Zaitsev: Nonlinear elastic properties of microinhomogeneous hierarchically structured media. *Acoust. Physics* 43 (1997) 594–599.

[36] I. Y. Belyaeva, V. Y. Zaitsev: The limiting value of the parameter of elastic nonlinearity in structurally inhomogeneous media. *Akust. Zhurnal* 44 (1998) 731–737. [Engl. Transl.: Acoust. Phys. 44(6), (1998)].

[37] V. Y. Zaitsev, V. E. Nazarov: On the frequency-independent acoustic Q-factor of microinhomogeneous media. *Acoustics Letters* 21 (1997) 11–15.

[38] V. Zaitsev: Anomalously high elastic nonlinearity and the frequency-independent Q-factor as complementary properties of microinhomogeneous solids. CD-proceedings of the International Conference "Forum Acusticum 99" - Joint Meeting ASA/EAA/DEGA, 15–19 March 1999, Berlin, Germany, 1999.

[39] V. Y. Zaitsev, V. E. Nazarov, A. E. Shul'ga: On dispersive and dissipative properties of microinhomogeneous media. *Acoust. Physics* 46 (2000) 295–301.

[40] V. Zaitsev, P. Sas: Elastic moduli and dissipative properties of microinhomogeneous solids with isotropically oriented defects. *Acustica-Acta Acustica* 86 (2000) 216–228.

[41] V. E. Gusev, H. Bailliet, P. Lotton, M. Bruneau: Interaction of counterpropagating acoustic waves in media with nonlinear dissipation and in hysteretic media. *Wave Motion* 29 (1999) 211–221.

[42] J. B. Walsh: Seismic wave attenuation in rock due to friction. *J. Geophys. Research* 71 (1966) 2591–2599.

[43] G. M. Mavko, A. Nur: The effect of nonelliptical cracks on the compressibility of rocks. *J. Geophys. Research* 83 (1978) 4459–4468.

[44] A. N. Tutuncu, M. M. Sharma: The influence of fluids on grain contact stiffness and the frame moduli of sedimentary rocks. *Geophysics* 57 (1992) 1571–1582.

[45] V. L. Vinickii, N. V. Kuhtarev: *Dynamicheskaya holografiya (dynamic holography)*. Naukova dumka, Kiev, 1983, 126 pp. (in Russian).

[46] I. Sneddon: *Fourier transforms*. Pergamon, 1951.

[47] J. C. Savage: Thermoelastic attenuation of elastic waves by cracks. *J. Geophys. Research* 71 (1966) 3929–3938.

[48] L. D. Landau, E. M. Lifshitz: *Theory of elasticity*. Pergamon, 1986.

[49] B. Armstrong-Helouvry, P. Dupont, C. C. De Wit: A survey of models, analysis tools and compensation methods for the control of machines with friction. *Automatica* 30 (1994) 1083–1138.

[50] G. Zames, N. A. Shneydor: Dither in nonlinear systems. *IEEE Trans. on Automatic Control* AC21 (1976) 660–667.

[51] V. E. Nazarov: Elastic waves in media with strong acoustic nonlinearity. Dr.Sc. Thesis, Institute of Applied Physics, Russian Acad. Sc., Nizhny Novgorod, Russia, 1996.

[52] K. Winker: The effects of pore fluids and frictional sliding on seismic attenuation. Ph.D. Thesis, Stanford University, Calif., USA, 1979.

[53] V. Zaitsev, V. E. Nazarov, I. Y. Belyaeva: The dynamical equation of state of microinhomogeneous materials and the frequency dependence of their elastic nonlinearity. *Akust. Zhurnal* 46 (2000) (accepted). [Engl. Transl.: Acoust. Phys. 46, (2000, accepted)].

[54] S. V. Zimenkov, V. E. Nazarov: The dependence of damping of ultrasound by sound in annealed copper on the frequency of the sound. *Akust. Zhurnal* 38 (1992) 778–779. [Engl. Transl.: Sov. Phys. Acoust., 38(4), (1992)].

[55] A. S. Korotkov, A. M. Sutin: Modulation of ultrasound by vibrations in metal constructions with cracks. *Acoustics Letters* 18 (1994) 59–62.

[56] A. E. Ekimov, I. N. Didenkulov, V. V. Kazakov: Nonlinear acoustic phenomena in a rod with a crack. Proc. 3-rd Int. Conf. "Acoustical and Vibratory Surveillance Methods and Diagnostic Techniques", October, 1998, Senlis, France, 1998. 481–489.

[57] V. Y. Zaitsev, P. Sas: Nonlinear response of a weakly damaged metal sample: a dissipative mechanism of vibro-acoustic interaction. *Journal of Vibration and Control* 6 (2000) (accepted).